



Research Applications of Positron Emission Tomography/Magnetic Resonance (PET/MR) Imaging in Cerebrovascular Diseases

Yaqin Hou, Yue Zhang, Fan Fu, Miao Zhang, Xiang Li, and Jie Lu

Cerebrovascular disease is currently one of the foremost diseases in the world with respect to incidence, disability, and fatality rates. As China gradually transitions to an aging society, the incidence rate of cerebrovascular disease has increased each year, accompanied by a trend toward a younger age at onset. The most common type of cerebrovascular disease is ischemic, accounting for 75–90% of all cases. Ischemic cerebrovascular disease has a complicated etiology and complex pathological mechanisms. It generally results from ischemic and hypoxic brain tissue caused by intracranial vessel wall lesions, alterations in blood components, or changes in hemodynamics, leading to brain dysfunction, or even the necrosis and softening of brain tissue. Clinically, this manifests as transient ischemic attacks, reversible ischemic neurological deficits, or cerebral infarctions, subsequently leading to corresponding neurological signs and symptoms. Although most cases of ischemic cerebrovascular disease are non-fatal, the resulting disability rate is very high; therefore, this disease has remained a major research topic in the

field of medicine worldwide. The rapid development of neuroimaging, in particular, the ability of functional imaging techniques to not only display morphological changes but also provide information on cerebral blood flow, metabolism, and other aspects, has played a crucial and even decisive role in the early diagnosis and appropriate treatment of ischemic cerebrovascular disease. In this chapter, we will focus on the research advances of MRI, PET, and PET/MR as they relate to the etiology, pathophysiology, treatment decision-making, and efficacy evaluation of ischemic cerebrovascular disease.

12.1 Research Applications of MRI in Cerebrovascular Diseases

During the pathophysiological process of cerebrovascular disease, cellular and histological damage is preceded by changes in cerebral hemodynamics, which is constantly in a state of dynamic flux. Therefore, these changes in cerebral hemodynamics and the associated changes in brain function are of critical importance to research on the early signs, diagnosis, and pathogenic mechanisms of cerebrovascular disease. Functional MRI (fMRI) techniques include diffusion-weighted imaging (DWI), diffusion kurtosis imaging (DKI), diffusion tensor imaging (DTI), perfusion-weighted imaging (PWI), arterial spin labeling (ASL), magnetic resonance

Y. Hou · Y. Zhang · F. Fu · M. Zhang · J. Lu (✉)
Department of Radiology and Nuclear Medicine,
Xuanwu Hospital, Capital Medical University,
Beijing, China

X. Li
Department of Biomedical Imaging and Image-
Guided Therapy, Medical University of Vienna,
Vienna, Austria

spectroscopy (MRS), and blood-oxygen-level-dependent (BOLD) imaging. These techniques can display focal cerebral ischemia at a very early stage, track the course of white matter fibers, reflect the perfusion status of brain tissues, display tissue metabolic and biochemical changes, determine the location of brain functional areas, and reveal whole-brain functional connectivity and functional networks.

12.1.1 Research Applications of DWI in Cerebrovascular Diseases

DWI involves the detection of the diffusion movement of water molecules in human tissues. By measuring the signal intensities before and after the application of diffusion-sensitivity gradient magnetic fields, we can calculate the tissue diffusion coefficient, known as the apparent diffusion coefficient (ADC), and therefore quantify the diffusion rate of water molecules in tissues.

DWI is primarily utilized in the diagnosis of acute and hyperacute cerebral infarction. Due to the occurrence of cytotoxic edema in the early stages of cerebral ischemia, the intracellular

water content increases, causing increased cellular swelling and decreased extracellular space, in turn decreasing the diffusion rate of water molecules in the area of infarction. Therefore, at 30 min after the onset of cerebral ischemia, abnormal hyperintensities can be observed in DWI, appearing as hypointensities on the ADC map (Fig. 12.1). ADC values can be used to monitor lesion growth and progression, with areas of cerebral infarction showing a significant reduction in ADC values during the acute stage, followed by the pseudo-normalization or even elevation of ADC values in the late subacute and chronic stages. DWI enables the accurate delineation of the extent and degree of cerebral infarction, the prediction of disease severity, and the dynamic evaluation of therapeutic efficacy. In conventional T_2 -weighted imaging (T_2 WI), cerebral infarcts appear as homogeneous hyperintensities, which does not allow for the distinction between old and new lesions; whereas in DWI, acute lesions appear as hyperintensities and chronic lesions as hypointensities, which are easily differentiated. Furthermore, DWI can also improve the detection rate of small ischemic lesions, especially small subtentorial lesions that

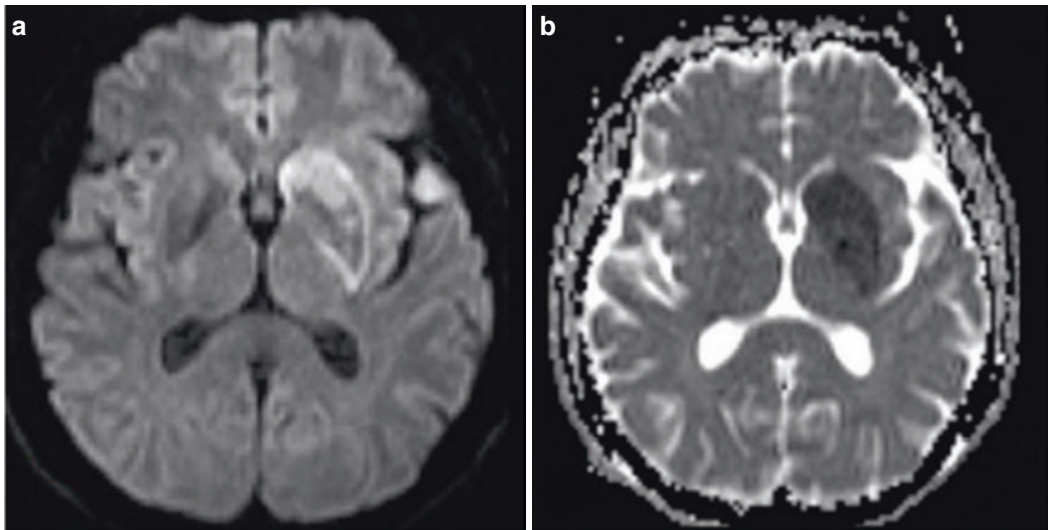


Fig. 12.1 Hyperacute cerebral infarction. A 48-year-old male patient with sudden weakness and numbness in his right limbs. Transverse DWI shows hyperintense signals

in the left basal ganglia (a). Transverse ADC mapping shows hypointense signals in the left basal ganglia (b)

are easily missed in conventional computed tomography (CT) and MRI sequences (Fig. 12.2).

DKI is an extension of DWI. Traditional DWI is based on the normal distribution of diffusion in water molecules, whereas DKI shows the non-normally distributed diffusion of water molecules in tissues. Therefore, DKI is able to provide a more accurate delineation of changes in tissue microstructures and allows for the early evaluation of the extent of any cerebral infarct. Additionally, DKI can simultaneously obtain both DKI and DWI parameters, which primarily include mean kurtosis (MK), mean diffusivity (MD), and ADC values. The size of the MK depends on the complexity of the tissue structures rather than their spatial direction, and can therefore more accurately display the extent of cerebral infarcts and their associated internal microstructural changes. MD is the mean ADC

value of the three orthogonal directions and is primarily used to measure the diffusion rate of water molecules, in turn reflecting cellular size and integrity. Compared to ADC, MD provides a more comprehensive reflection of the rate of diffusion movement. In acute cerebral ischemia, MD reflects the extent of cytotoxic edema in tissues, while MK is more sensitive to the disintegration of cytoskeletal structures and mitochondrial swelling. Therefore, regions with mismatched MK and MD abnormalities represent the ischemic penumbra, whereas matched regions represent the area of infarction and severe cell damage (Fig. 12.3). DKI is more accurate than DWI in the diagnosis of early cerebral infarction, and the comparative analysis between the two may have significant implications in both determining the ischemic penumbra and improving patient prognosis. Furthermore, DKI can also

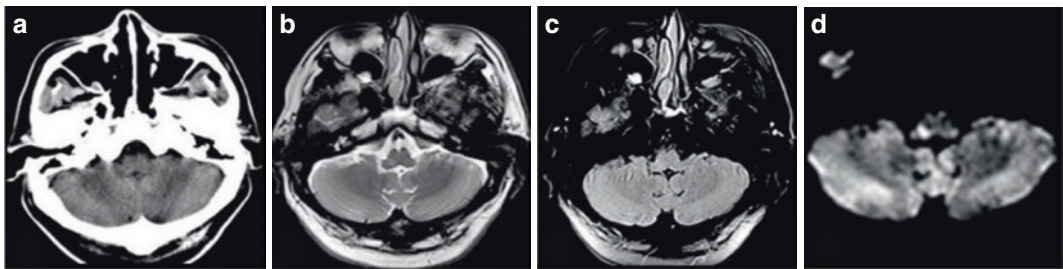


Fig. 12.2 Acute medullary infarction. A 46-year-old female patient who presented with numbness and weakness in her left limbs for 4 h. Transverse plain CT scan shows no abnormalities (a). Transverse T₂WI shows slight hyperintensity in the right dorsolateral medulla oblongata

(b). Transverse FLAIR shows suspicious slight hyperintensity in the right dorsolateral medulla oblongata (c). Transverse DWI shows hyperintensity in the right dorsolateral medulla oblongata (d)

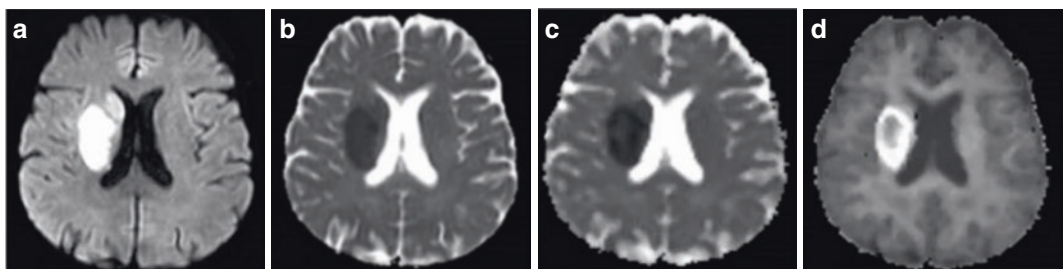


Fig. 12.3 Acute right periventricular cerebral infarction. A 55-year-old male patient who presented with left-sided sensory disturbances for 8 h. Transverse DWI shows homogeneous hyperintense signals in the right periventricular area (a). Transverse ADC mapping (b) and MD

(c) show homogeneous hypointense signals. Transverse MK shows heterogeneous hyperintense signals in the right periventricular area, mismatched with the extent of the lesion as determined by DWI, ADC, and MD (d)

facilitate the more in-depth analysis of pathological mechanisms at the microscopic level, which can provide useful information for more targeted clinical treatments. Although research on the utilization of DKI in ischemic stroke is currently in its infancy, DKI is ideal for widespread clinical use due to its minimal hardware requirements and short scan time; relevant research will provide new ideas for the diagnosis and treatment of cerebral infarctions.

12.1.2 Research Applications of DTI in Cerebrovascular Diseases

DTI parameters can reflect the integrity of neuronal membrane and nerve fiber myelination. These indicators do not exhibit significant changes during the acute phase of ischemic stroke but are altered significantly in the subacute and chronic phases, due to the loss of fractional anisotropy (FA) caused by the destruction of cellular and/or myelin structures. Despite the extensive utilization of DWI in the evaluation of acute ischemic stroke, its use in chronic ischemic injuries is still limited. In contrast, DTI can provide information on evolving stroke that cannot be acquired using DWI, and is therefore useful for predicting the severity of ischemic injury and patient prognosis in the early stages of ischemic stroke. Studies have found that after the onset of cerebral infarction, dynamic and predictable changes in FA and MD values can be observed over the course of the disease. More specifically, there is a continuous decrease in FA values after cerebral infarction, primarily due to the myelinolysis and axonal disintegration of white matter fibers superior and inferior to the infarct, as well as glial proliferation in the peri-infarct area, leading to the impaired integrity of nerve fibers and a reduction in structural directionality. The trend and timing of changes in FA values concur with Wallerian degeneration. MD values, on the other hand, show an initial decrease followed by a gradual increase and can be attributed to the cytotoxic edema found in acute cerebral infarction, which causes continuous restricted diffusion, significantly reducing the MD values, in turn reflecting

the degree of diffusion. When cytotoxic edema progresses to vasogenic edema, there is an increase in extracellular water, elevation of total tissue water content, further exacerbation of cellular damage, and collapse of cellular membrane structure, which produces a large amount of cell debris. This increases intracellular viscosity and causes an elevated level of free diffusion, leading to a gradual rise in MD values. The subsequent necrosis and liquefaction in the area of infarction further enhances the free diffusion of water molecules, resulting in abnormally high MD values. Monitoring the post-infarction changes in DTI parameters can deepen our understanding on the pathophysiological evolution of cerebral infarction and enable a more accurate staging of this disease. The severity of early-stage Wallerian degeneration is related to the recovery of the patient's neurological function. That is, patients with more significant early-stage pyramidal tract degeneration experience more severe neurological impairment, especially with respect to the patient's motor functions. Based on the extent of Wallerian degeneration in the patient's pyramidal tract distal to the lesion, it is possible to predict the long-term recovery of motor function. This is useful for the early determination of patient prognosis, which in turn allows the formulation of an appropriate treatment plan in order to promote functional recovery.

Diffusion tensor tractography (DTT) is an imaging method that involves the use of diffusion tensor data to determine the seed region on the basic images, which are then subjected to fiber tracking or tractography. DTT can accurately determine the anatomical structure of white matter fiber bundles and describe the spatial relationship between the lesion and specific fiber bundles. DTT represents an expansion of imaging techniques from the basics of early diagnosis and evaluation of lesion characteristics to the more involved direct evaluation of relationships between the lesion and key white matter fiber bundles, to predict patient prognosis and functional recovery. The rehabilitation of patients after cerebral infarction depends, to a large extent, on the recovery of limb motor function. Therefore, understanding the degree of damage

to the motor tracts after a cerebral infarction is useful for accurately assessing the recovery of motor function. The corticospinal tracts are the largest of the descending pyramidal tracts primarily responsible for controlling voluntary limb movements, and they play a pivotal role in the recovery process of motor functions in stroke patients. DTT can be used to display the spatial relationships between the cerebral infarct and the corticospinal tracts and serve as a reference for predicting motor outcome in several situations.

1. Patients with corticospinal tracts which run adjacent to the infarct area exhibit virtually unaffected motor function, although some patients experience mild limb numbness and weakness, which can be explained by the space-occupying effects of transient peri-infarct edema (Fig. 12.4).
2. Among patients whose corticospinal tracts are compressed or contorted, some of whom experienced significant improvements in motor dysfunction within a short period of time, and essentially recovered during the chronic phase. This may be due to the space-occupying effects caused by the hyperemia and edema of the infarct itself and surrounding brain tissues in the early stages, which led to the contortion and compression of white matter fiber bundles. However, after the hyperemia and edema have subsided and the lesion has decreased in size, the compression

of the white matter fiber bundles resolved, leading to significant improvements in the patient's motor dysfunction (Fig. 12.5).

3. Patients in whom a small number of lesions have led to the partial interruption of the corticospinal tracts may still experience a good recovery in motor function, which may be related to the compensation of unaffected motor fibers.
4. In cases where most or all of the corticospinal tracts are involved, causing the majority of fiber bundles to be interrupted or damaged, patients present with severe motor impairments in the acute phase, although some patients may gain some degree of motor function recovery through mechanisms such as the remodeling of white matter fiber bundles and functional compensation. However, such patients experience a slower recovery in motor function compared to patients without corticospinal tract involvement (Fig. 12.6).

Although most patients with cerebral infarction involving the complete corticospinal tract have a poorer prognosis than those with partial involvement, long-term follow-up observations have found that further recovery in motor function is still possible. It is generally believed that motor function recovery in the early post-infarction stages is primarily associated with improvements in lesion ischemia and edema, whereas in the later stages of recovery, it is

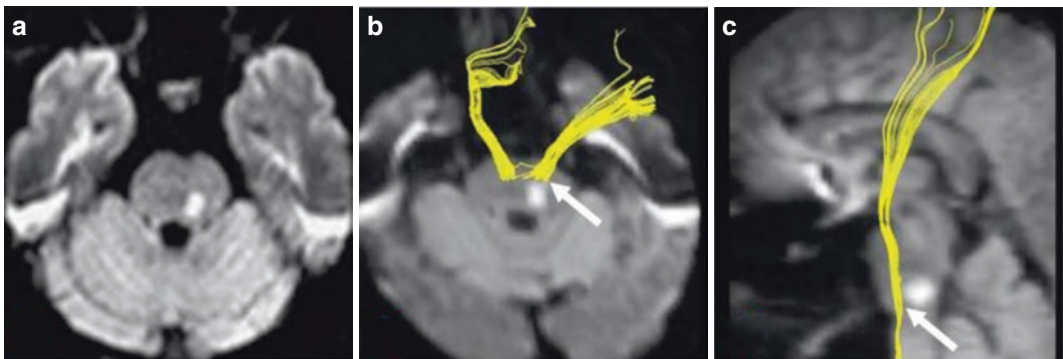


Fig. 12.4 Left pontine infarction. A 57-year-old male patient who presented with numbness and weakness of the right limbs for 1 d. The patient's limb motor dysfunction recovered significantly after 2 weeks. Transverse DWI

shows left pontine infarction (a). Transverse (b) and sagittal (c) MRI show that the left corticospinal tracts are located anterior to the infarct, exhibiting good continuity, without compression or interruption (arrows)

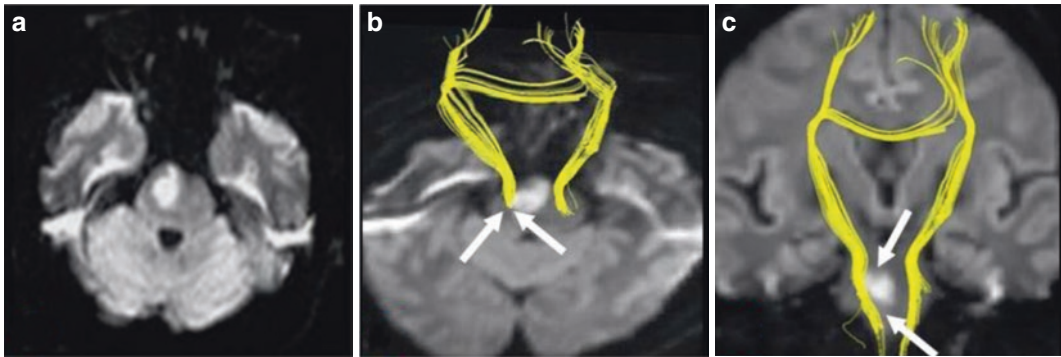


Fig. 12.5 Right pontine infarction. A 59-year-old male patient who presented with left limb weakness and slurred speech for 2 d. The patient recovered after 3 months of routine medical treatment and rehabilitation training. Transverse DWI shows right pontine infarction (a).

Transverse (b) and coronal (c) MRI show that the right corticospinal tracts are immediately adjacent to the infarct, exhibiting compression and contortion but without significant interruption (arrows)

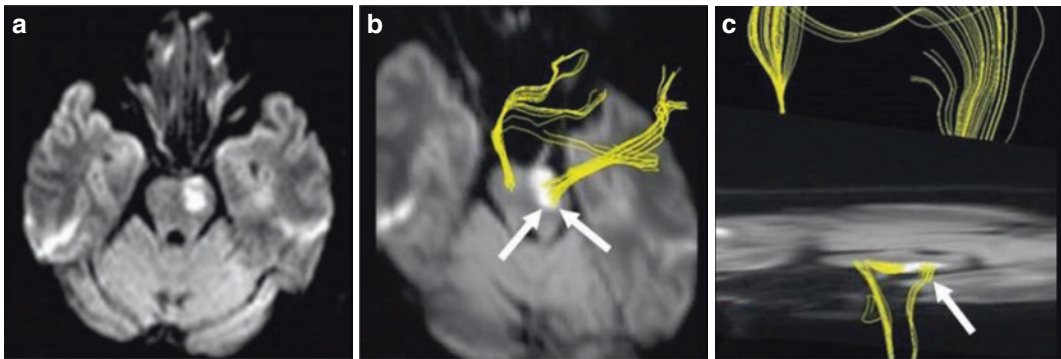


Fig. 12.6 Left pontine infarction. A 62-year-old female patient who presented with right limb weakness and slurred speech for 2 d. Motor dysfunction remained after 3 months of routine medical treatment and rehabilitation training. Transverse DWI shows left pontine infarction

(a). Transverse (b) and sagittal (c) MRI show that the left corticospinal tracts pass through the infarct, and the majority of fiber bundles have been interrupted, with only a few fiber bundles remaining inferior to the level of the infarct (arrows)

closely related to functional brain reorganization. Research has shown that multiple cortical areas and conduction pathways are involved in the reorganization of motor function. In addition to the primary motor cortex, the premotor area of the frontal lobe, the supplementary motor area of the insula, and the medial surfaces of the cerebral hemispheres are all associated with motor functional recovery and have nerve fiber connections with the spinal cord. Under normal circumstances, these areas of the brain and their associated descending pathways are in an inhibited state. When the primary motor cortex and its descending pathways are damaged, this inhibi-

tion is removed, and the resulting compensatory effects enable patients to restore their motor functions.

The corpus callosum is the largest bundle of commissural fibers connecting the two cerebral hemispheres. In healthy individuals, the callosal fibers are generally in an inhibited state to maintain the functional balance of the cerebral motor cortex between the two hemispheres. After a unilateral ischemic stroke occurs in the cerebral hemisphere, the inhibition on the callosal fibers is removed, allowing the nerve fibers from the contralateral corticospinal tract to traverse to the affected side via the corpus callosum, and then

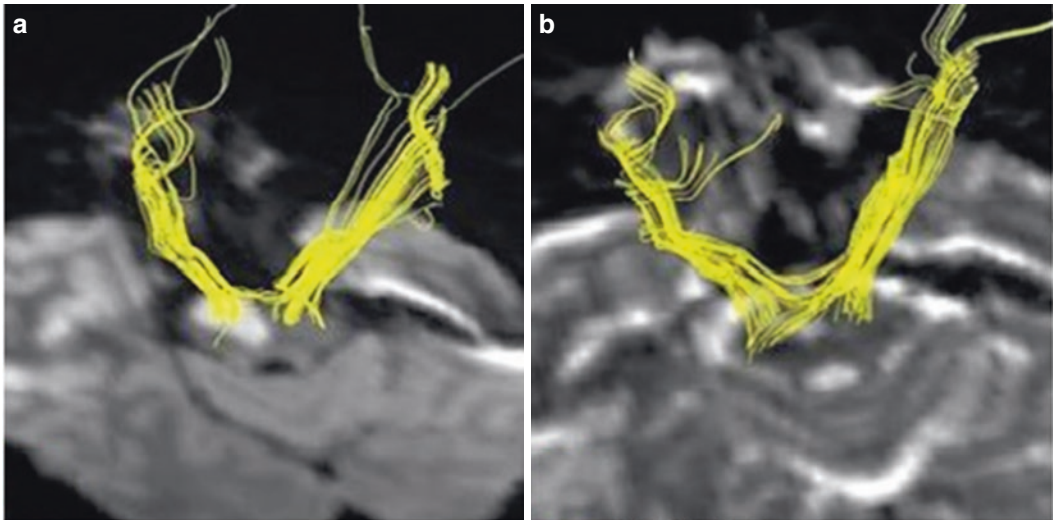


Fig. 12.7 Right pontine infarction. A 60-year-old male patient who presented with left hemiplegia and dizziness. Transverse DWI shows right pontine infarction, and transverse DTT shows that nearly the entire right corticospinal

tract has passed through the infarct (a). At 180 d after disease onset, DTT shows part of the contralesional fiber bundles crossing over to the ipsilesional side and descending laterally along the infarct (b)

descend along the infarct to compensate the function of the damaged corticospinal tract (Fig. 12.7). The contralateral corticospinal tract can also project multiple pontine association fibers to the affected side, even extending up to the motor cortex of the affected hemisphere to compensate for impaired motor functions. Jang et al. performed a DTT study on 40 patients with an infarction of the corona radiata, who were classified according to DTT findings into three types: (1) Type A patients did not have transcallosal fibers originating from contralesional corticospinal tracts; (2) Type B patients had transcallosal fibers originating from contralesional corticospinal tracts that terminated at the corpus callosum or ascended to the cortex of the affected cerebral hemisphere; and (3) Type C patients had transcallosal fibers that projected to the ipsilesional side and descended along the infarct. Patients with severe motor impairment were predominantly type C, implying that severe damage to the motor pathway can remove the inhibited state of dormant fibers, in an effort to compensate for the damaged nerve fibers and restore the patient's motor functions. Damaged corticospinal tracts can also undergo reorganization in the peri-infarct area to restore the patient's motor function. The mecha-

nism underlying this functional recovery is thought to involve the axonal regeneration, dendritic collateral branch formation, and altered synaptic thresholds of unaffected cells around the infarct, mobilizing reserved neural function, rebuilding neural networks, and achieving functional plasticity, subsequently compensating for the brain functions of the affected regions.

12.1.3 Research Applications of Brain Perfusion MRI in Cerebrovascular Diseases

Brain perfusion MRI includes dynamic susceptibility contrast (DSC)-PWI and arterial spin labeling (ASL). DSC-PWI involves the use of rapid scanning and the intravenous bolus injection of contrast agents, so that the changes in tissue magnetic susceptibility caused by the contrast agent lead to changes in MRI signals, which in turn can be used to evaluate the hemodynamics of the brain tissue. Using this imaging technique, parameters such as regional cerebral blood flow (rCBF), relative cerebral blood volume (rCBV), mean transit time (MTT), and time-to-peak (TTP) can be calculated. PWI is highly sensitive

to early cerebral ischemia, detecting abnormalities even earlier than DWI. Therefore, performing PWI and DWI at the same time is useful for determining the presence of an ischemic penumbra. During hyperacute cerebral infarction, a larger region of abnormal perfusion is delineated PWI compared to the region of abnormal DWI signals (i.e., the cerebral infarct area), suggesting the presence of an ischemic penumbra. This sign can be used to assist in the selection of patients for thrombolytic therapy, so as to minimize the infarct area, implement individualized therapy for cerebral infarction, and evaluate the efficacy of thrombolytic therapy (Fig. 12.8). The utilization of PWI in patients with chronic middle cerebral artery/internal carotid artery stenosis or occlusion can facilitate the discovery of cerebral ischemic lesions that cannot be detected using conventional MRI. These lesions manifest as delayed TTP and MTT, without significant changes in CBF and CBV, or as normal CBF with slightly elevated CBV. These findings imply that cerebral ischemia induces compensatory cerebrovascular dilation, which decreases circulatory resistance and reduces blood flow velocity and also establishes collateral circulation. Together,

these compensatory mechanisms maintain CBF within the normal range (Fig. 12.9). However, compared to healthy individuals, these patients take a longer time for blood supply to reach the ischemic area, decreasing the effective uptake rate of CBF, and diminishing the compensatory and stress response abilities of the cerebral vessels. Therefore, these ischemic areas are at high risk for cerebral infarction and are useful for screening high-risk groups for stroke and performing preventative treatment.

Compared to conventional DSC-PWI, ASL is a brain perfusion imaging technique that does not require the injection of gadolinium-based contrast agents, and as such can be used in patients with renal dysfunction. ASL can be divided based on the labeling method into the following four types: continuous ASL, pulsed ASL, pseudo-continuous ASL, and velocity-selective ASL. Other techniques include territorial ASL and ASL-angiography. ASL can only produce a single parameter, CBF; therefore, it is less effective at evaluating the infarct core during acute cerebral infarction compared to DWI and PWI but is equally sensitive at displaying changes in early cerebral ischemia

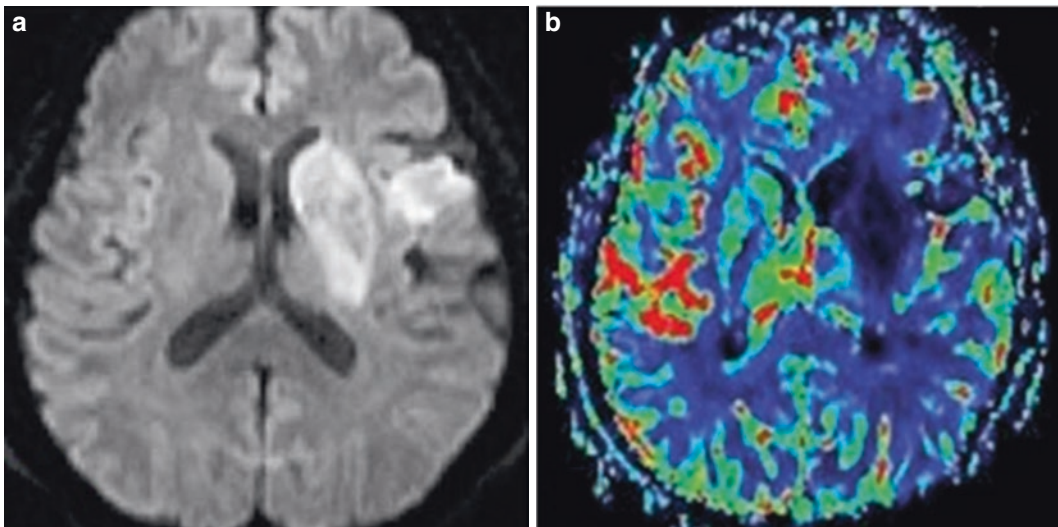


Fig. 12.8 Acute cerebral infarction of the left basal ganglia and left temporal lobe. A 62-year-old male patient who presented with weakness in his right limbs for 3 h. Transverse DWI shows acute cerebral infarction of the left basal ganglia and left temporal lobe (a). Transverse PWI

shows hypoperfusion of the middle cerebral artery territory, covering a larger area than the extent of DWI hyperintensity (b). Therefore, there is a mismatch between CBF and DWI, which implies the presence of an ischemic penumbra

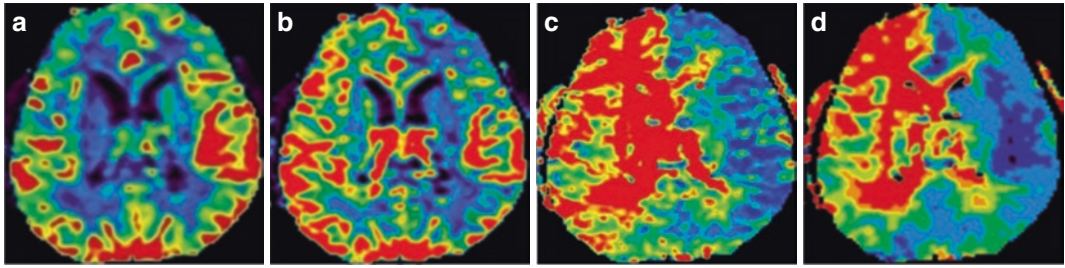


Fig. 12.9 Right internal carotid artery occlusion. A 63-year-old male patient whose MRI shows bilateral periventricular lacunar infarction. Transverse PWI shows roughly symmetric CBF between the bilateral cerebral

hemispheres (a), as well as slight CBV elevation (b), delayed MTT (c), and delayed TTP (d) in the right cerebral hemisphere

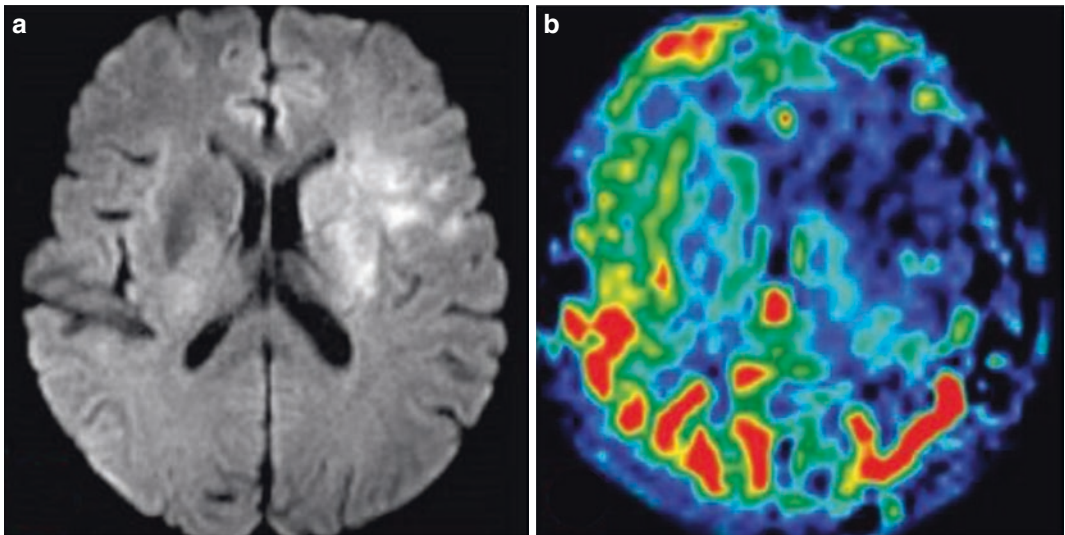


Fig. 12.10 Acute cerebral infarction of the left frontal lobe and left basal ganglia. A 72-year-old female patient who presented with weakness in her right limbs and aphasia for 1 h. Transverse DWI shows acute cerebral infarction

of the left frontal lobe and left basal ganglia (a). Transverse ASL shows reduced CBF in the left middle cerebral artery territory (b)

(Fig. 12.10). Mirasol et al. found that in the assessment of acute ischemic stroke, the regions with decreased CBF as delineated by ASL showed good concordance with the hypoperfused regions determined by DWI-PWI and CT perfusion imaging. As for patients with chronic middle cerebral artery/internal carotid artery occlusion or stenosis whose ischemic lesions cannot be detected using conventional MRI, ASL can be utilized to display abnormal cerebral perfusion in the areas ipsilateral to the affected blood vessels (Fig. 12.11).

During ASL scans, blood labeled by magnetic inversion reaches the capillaries after a period of time, at which point image acquisition can be performed. The interval between labeling and acquisition is known as the post-labeling delay (PLD) and is a key parameter of ASL. The selection of the PLD can affect the determination of CBF and the assessment of perfusion. By adopting two different PLDs when studying chronic ischemic cerebrovascular disease, we can achieve a better evaluation of actual cerebral perfusion levels. More specifically, a shorter PLD can more

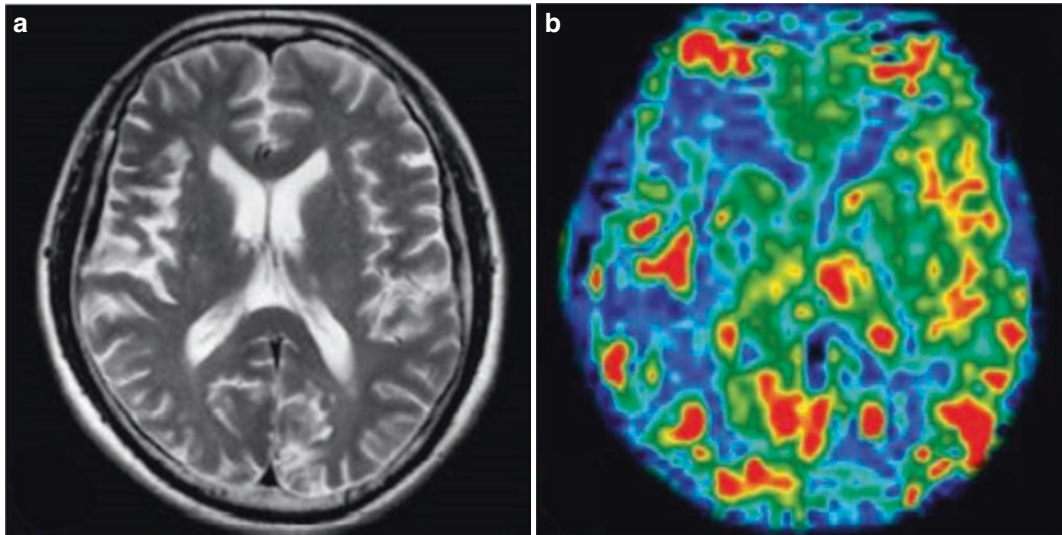


Fig. 12.11 Severe stenosis of the right middle cerebral artery. A 62-year-old male patient, in whom severe stenosis of the right middle cerebral artery had been discovered

for 1 year. Transverse T₂WI shows no clear abnormalities (a). Transverse ASL shows reduced CBF of the right middle cerebral artery territory (b)

easily detect perfusion abnormalities caused by large-vessel stenosis, whereas a longer PLD can more accurately assess actual perfusion levels, owing to the longer time required by collateral circulation pathways than the direct blood supply from normal arteries. Therefore, the contrast between the CBF images derived from these two PLDs can reflect the status of cerebral perfusion compensation or the level of cerebrovascular reserve, which is of practical significance in clinical settings for the accurate assessment of ischemic levels and determination of prognosis. Using ischemic moyamoya disease in children as an example, performing scans with two different PLDs enables the level of perfusion compensation to be assessed more accurately, which can then be applied to the formulation of individualized treatment plans (Fig. 12.12). Lyu et al. performed ASL using two different PLDs to differentiate between antegrade and collateral blood flow in patients with middle cerebral artery stenosis and proposed the possibility of quantifying collateral blood flow using ASL.

Territorial ASL, also known as vessel-selective ASL, involves labeling the blood in specific blood vessels to observe the compensatory effects of collateral vessels on the territory of occluded

vessels following a proximal large-vessel occlusion. This technique is now widely used in the determination of collateral blood flow in patients with carotid artery stenosis and moyamoya disease (Fig. 12.13).

12.1.4 Research Applications of MRS in Cerebrovascular Diseases

MRS is an effective technique for the non-invasive *in vivo* evaluation of tissue metabolism. The progressive decline, or even disappearance, of intralésional N-acetylaspartate (NAA) can be observed in acute cerebral infarction, while patients with a more significant decrease in NAA levels have poorer prognosis. In contrast, the decline in the choline (Cho) and creatinine (Cr) peaks tend to be less significant than that of NAA. Lactate (Lac) is a product of anaerobic glycolysis that cannot be detected in normal brain tissues. Therefore, elevated Lac concentrations imply that tissue ischemia and hypoxia have resulted in impairments in normal aerobic metabolism. In fact, Lac can be detected using ¹H-MRS a few minutes after the onset of cerebral ischemia, following which Lac increases rapidly,

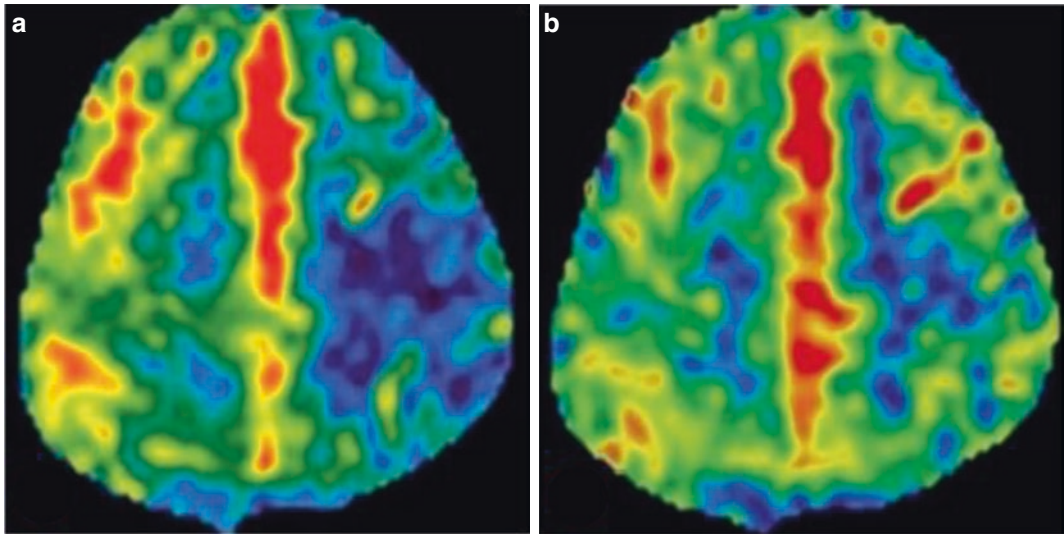


Fig. 12.12 Moyamoya disease. A 9-year-old male patient. Transverse ASL with PLD = 1.5 s shows reduced CBF in the left frontoparietal lobe (a). Transverse ASL

with PLD = 2.5 s shows a smaller extent of CBF reduction in the left frontoparietal lobe (b)

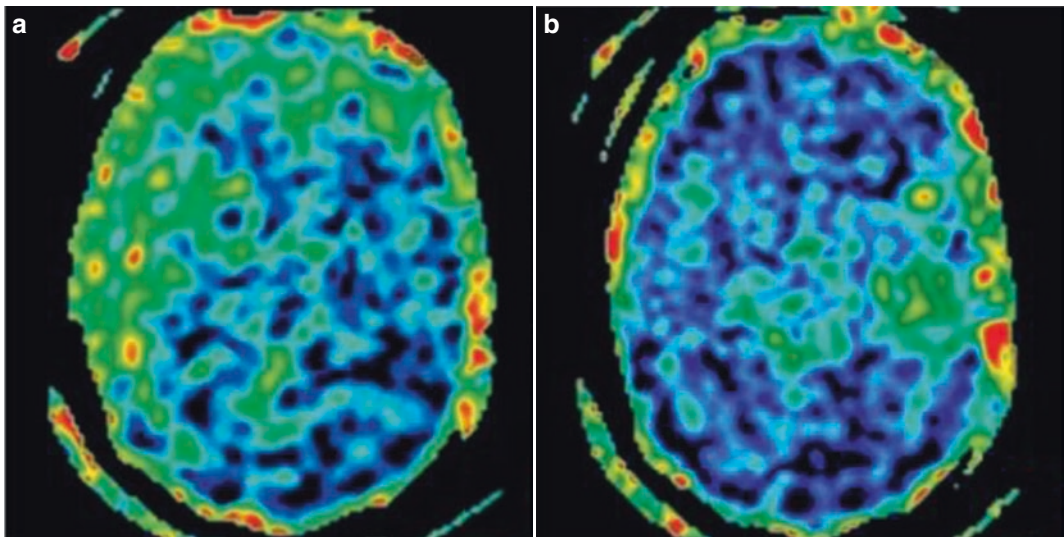


Fig. 12.13 Severe stenosis of the right internal carotid artery. A 64-year-old male patient. MRI performed with selective labeling of the right internal carotid artery. Transverse territorial ASL shows perfusion defects in the right frontoparietal lobe (a). Selective labeling of the left

internal carotid artery. Transverse territorial ASL shows normal perfusion in the left hemisphere, while perfusion can be observed in the right prefrontal lobe, suggesting compensatory blood supply by the left internal carotid artery to the right frontal lobe (b)

reaching its peak during the hyperacute phase. Therefore, Lac is considered a sensitive marker in the early stages of cerebral infarction (Fig. 12.14). $^1\text{H-MRS}$ is a valuable technique for differentiating between the area of cerebral

infarction and the ischemic penumbra. In acute cerebral infarction, the extent of Lac presence is often larger than the infarct area as delineated by conventional MRI. Therefore, a region with normal MRI findings and normal or slightly reduced

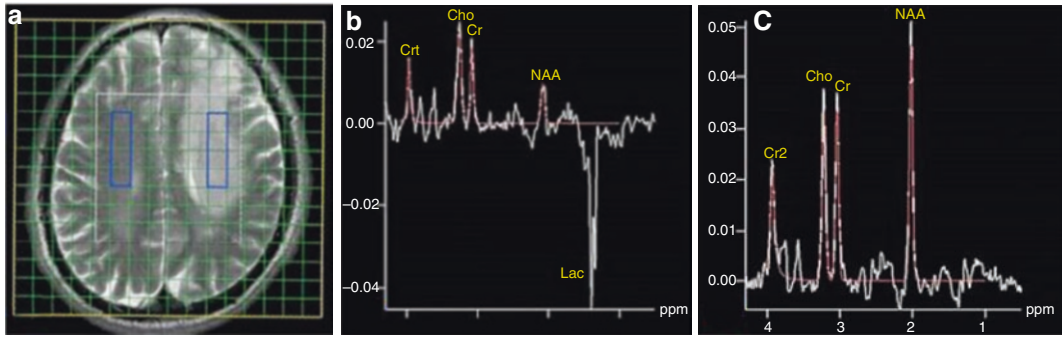


Fig. 12.14 ^1H -MRS localization. Transverse $T_2\text{WI}$ shows a large area of infarct in the left centrum semiovale. MRI-based ^1H -MRS localization map: four symmetric voxels were selected at the lesion center and corresponding contralateral site (a). The infarct ^1H -MRS curve shows

a significant decrease in NAA, varying extents of decreases in Cho and Cr, and a deep inverted Lac peak at 1.33 ppm (b). ^1H -MRS of normal contralateral brain tissues shows the NAA, Cho, and Cr peaks, and the absence of a Lac peak (c)

NAA, but with the presence of a Lac peak, can be regarded as an ischemic penumbra. Additionally, the Lac/NAA ratio can also be used to determine the infarct area, where a ratio > 1.0 denotes the infarct area, and < 1.0 indicates the non-infarct area. However, further investigations are needed to determine whether the degree of NAA and Lac changes can be used to discriminate among the infarct core, ischemic penumbra and benign hypoperfusion.

For patients with chronic cerebral ischemia accompanied by intra- and extracranial large-vessel stenosis or occlusion, but are in the compensatory phase, the level of cerebral ischemia is often not completely consistent with the degree of vascular stenosis, due to factors such as compensatory blood supply via collateral circulation. Therefore, conventional imaging techniques often reveal no abnormalities, or only small lacunar infarcts, in most patients. At this point, patients may appear to have an essentially normal regional blood flow but may experience a decrease in cerebrovascular reserve capacity, and their brain tissue may have a reduced capacity for effective blood uptake, leaving the neurons in a functionally inhibited and hypometabolic state. The occurrence of acute decompensation at this point can easily cause a stroke, which can then lead to severe neurological impairments. A ^1H -MRS study on patients with chronic internal carotid artery/middle cerebral artery stenosis or occlusion found that

white matter which appeared without abnormal findings on conventional MRI exhibited metabolic abnormalities, manifesting as decreased NAA and increased Cho concentrations, with a Lac peak observed in some patients (Fig. 12.15). Although there is no fundamental difference in the cerebral metabolic changes detected by ^1H -MRS between chronic cerebral ischemia and infarction, their respective underlying mechanisms are not completely the same.

During cerebral infarction, neurons are subjected to irreversible damage, the number of cells is reduced, and NAA undergoes a progressive and irreparable decline. In chronic cerebral ischemia, however, the functional changes indicated by the decrease in NAA are relatively mild, while the neuronal structure of ischemic tissues remain intact, and may return to normal once blood circulation is restored. The mechanisms underlying ipsilesional Cho elevation are the same as those involved in the early stages of cerebral infarction. Both are the result of the degradation of cell membrane components in ischemic tissues and the release of large amounts of phosphatidylcholine, suggesting that metabolic abnormalities of the cell membrane may occur in the early stages of ischemia prior to the onset of cerebral infarction. This implies that such patients have sustained an ischemic brain injury, but the metabolic state of their brain tissue is still in the transitional stage toward cerebral infarction.

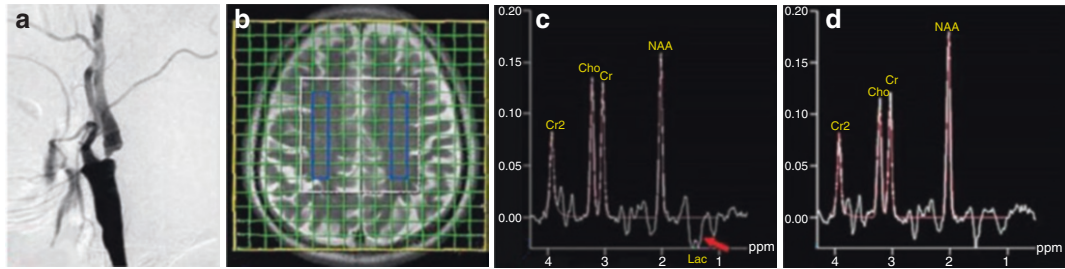


Fig. 12.15 Severe stenosis in the initial segment of the right internal carotid artery. A 45-year-old male patient who presented with recurrent left limb weakness for 3 years. Digital subtraction angiography shows severe stenosis in the initial segment of the right internal carotid artery (a). ^1H -MRS localization map: six symmetrical

voxels were selected each in the bilateral centrum semi-ovale (b). Right ^1H -MRS curve shows decreased NAA, increased Cho, and inverted Lac peak at 1.33 ppm (c) (arrow). Left ^1H -MRS curve at a symmetrical site shows the NAA, Cho and Cr peaks, and the absence of a Lac peak (d)

tion. The appearance of Lac is related to anaerobic glycolysis and the cellular infiltration of the infarcted area, and the presence of a Lac peak in patients with chronic cerebral ischemia can be attributed to the anaerobic glycolysis induced by the continuous hypoxic state of the brain tissue. Although such patients experience significantly lower levels of ischemia and hypoxia than those with cerebral infarction, the appearance of a Lac peak within a given region indicates that there is greater decrease in the cerebral perfusion of this particular area, which is more likely to develop cerebral infarction. Therefore, ^1H -MRS enables the early detection of high-risk areas for cerebral infarction, which can facilitate the accurate determination of the level of cerebral ischemia and patient's prognosis, while also providing a new evaluation method for patients in the compensatory phase of chronic cerebral ischemia.

12.1.5 Research Applications of BOLD Imaging in Cerebrovascular Diseases

BOLD imaging is primarily utilized in chronic cerebrovascular disease, especially in research of the mechanisms underlying post-infarction recovery. BOLD-fMRI studies on the recovery of motor function following cerebral ischemia revealed that hand movements performed by patients in the early stages after the onset of isch-

emia elicited extensive activation of the contralateral cerebral hemisphere. Furthermore, during the slow process of functional recovery, the extent of contralesional activation gradually decreased, whereas the ipsilesional hemisphere showed a tendency toward re-activation. The expansion of activated areas in the contralesional hemisphere was more common among patients with poor recovery, suggesting that activation in the contralesional hemisphere during the early stages of ischemia is not a key factor contributing to the recovery of motor function. This phenomenon is most likely due to the disinhibition of non-crossing corticospinal tracts in the contralesional hemisphere by the ipsilesional hemisphere. Following cerebral infarction, the non-injured, peri-infarct area in the ipsilesional cerebral hemisphere exhibits some degree of plasticity. Both human and animal studies have found that the peri-infarct area in the ipsilesional cerebral hemisphere can play a role in motor recovery. Additionally, one study found that the activation volume of the contralesional cerebellar hemisphere showed a positive linear association with the patient's recovery of motor function, implying that the cerebellum plays a mediating role in functional recovery from cerebral infarction. As with motor function, the recovery of language, sensory, cognitive, and other functions in patients with cerebral infarction is also closely related to the plasticity of brain tissues and the dynamic reorganization of neural networks. In BOLD-fMRI studies on patients with aphasia in the

recovery phase of cerebral infarction, it was found that language-related activation areas shifted from the left to the right cerebral hemisphere. This redistribution and reorganization indicate that the location of functional language areas of the cerebral cortex can be altered through sensory input, learning, and experience. The utilization of BOLD imaging in conjunction with simple language tasks is an effective method for evaluating the functional language status of aphasic patients with cerebral infarction. By monitoring the dynamic changes of the corresponding functional areas, as well as their relationship with the patient's functional recovery, we are able to gain a deeper understanding of the neural mechanisms of brain functional recovery.

However, patients with cerebral infarction often find it difficult to perform tasks and maintain task consistency. The general linear model (GLM) of BOLD imaging assumes that the patient's hemodynamic responses are normal, although the reduction in cerebral perfusion can lead to decreased BOLD signals. Additionally, the interconnectivity between brain areas is overlooked in task-based BOLD imaging. As research in functional brain imaging is carried out in greater depth, researchers have begun paying more attention to the information obtained by BOLD-fMRI in the resting state. Resting-state fMRI is beneficial to patients with cerebral infarction who are unable to perform tasks and is especially suitable for large-sample, long-term, longitudinal studies on patients with cerebral infarction. Extensive abnormalities can be observed in the functional networks of the brain after cerebral infarction. Current research has demonstrated that the functional motor network has been damaged in patients with cerebral infarction and that the improvement of motor function is closely linked with the remodeling of brain functions. Therefore, the analysis and evaluation of the whole-brain functional network are of crucial significance to studying the dynamic mechanisms underlying the process of motor function reorganization after cerebral infarction.

Carter et al. performed a cross-sectional study on patients with subacute stroke and found reduced interhemispheric functional connectivity

in the somatomotor network, including the bilateral primary motor cortices, supplementary motor area, secondary somatosensory cortex, cerebellum, thalamus, and putamen. Upper limb motor dysfunction was significantly correlated with the decreased interhemispheric functional connectivity of the bilateral primary motor cortices, but not with intrahemispheric functional connectivity. Furthermore, a follow-up study demonstrated that the decrease in the interhemispheric functional connectivity of the bilateral primary motor cortices can be detected within a few hours after the onset of cerebral infarction, and this functional connectivity was gradually strengthened with the recovery of motor function. Another study found that in the early stages of cerebral infarction, the interhemispheric functional connectivity between the bilateral primary motor cortices was more lateralized to the ipsilesional side. This asymmetry was greatest at 1 month after onset, and then gradually returned to normal levels, which was consistent with the redistribution of brain activation between the bilateral hemispheres as seen in task-based fMRI.

Longitudinal studies of patients with subcortical infarction revealed a decrease in functional connectivity between the ipsilesional primary motor cortex and relevant brain areas during the initial stages of recovery, whereas the functional connectivity of the ipsilesional thalamus and cerebellum with the main contralesional motor areas gradually decreased over the course of recovery. These findings indicate that the enhancement of the connectivity of the ipsilesional primary motor cortex is beneficial to motor function recovery. The dynamic changes in the functional connectivity between the ipsilesional primary sensorimotor cortex and the bilateral motor areas after cerebral infarction are significantly correlated with clinical motor function scores, suggesting that enhanced interhemispheric functional connectivity of the motor cortex may be the underlying brain mechanism of motor function recovery. By performing resting-state fMRI on patients with unilateral pontine infarction, Lu et al. showed that pontine infarction led to reduced functional connectivity in ipsilesional cerebrocerebellar motor pathways (decreased connectiv-

ity between ipsilesional motor cortex and contralesional cerebellum), as well as reduced functional connectivity in ipsilesional cerebro-cerebellar non-motor pathways (ipsilesional pre-frontal cortex and contralesional cerebellum). Such cerebrocerebellar functional disconnection demonstrates that anatomical neurocircuits are the biological basis of functional connectivity (Fig. 12.16). Additionally, resting-state fMRI can also be used to observe the impairments in the white matter functional connectivity of patients with cerebral infarction. Using white matter fMRI data, Wang et al. explored the changes in the white matter functional tensors of the sensorimotor system in patients with acute pontine infarction. They found that using fMRI and DTI for white matter tractography produced essentially the same results with respect to the morphology of patients' pontine-thalamic bundles. Furthermore, compared to healthy controls, patients with pontine infarction showed reduced functional tensor values of ipsilesional fiber bundles related to the thalamus-motor cortex, which were also significantly positively associated with the patients' upper limb motor scores at the six-month follow-up. These findings indicate that resting-state fMRI can uncover the dynamic patterns of repair in the white matter remodeling of patients with cerebral infarction, and may serve as a biomarker to predict the prognosis of motor patients' motor function.

Nevertheless, the vast majority of existing resting-state fMRI studies have utilized group analysis at the cohort level in the post-processing step, due to the low signal-to-noise ratio of BOLD data, which can be improved by implementing group analysis. Therefore, their findings can only reflect overall trends in functional brain networks, whereas inter-individual variability is discarded as noise, and as such does not meet the requirements for the individualized diagnosis and treatment of patients with clinical neurological diseases. Lu et al. challenged the post-processing models of traditional analysis methods and performed an in-depth analysis of the individual differences of functional connectivity in healthy adults. Their results revealed that inter-individual variability in functional connectivity is dependent on brain networks and evolution. Specifically, brain networks involved in higher-order cognition (language, control, and attention networks) exhibited significant inter-individual variability, whereas the primary visual, sensory, and motor cortices showed smaller inter-individual variability. Furthermore, the degree of variability in functional connectivity was positively correlated with the variability in sulcal depth, but not cortical thickness. The degree of variability in connectivity was also significantly negatively correlated with short-range connectivity but was significantly positively correlated with long-range connectivity (Fig. 12.17).

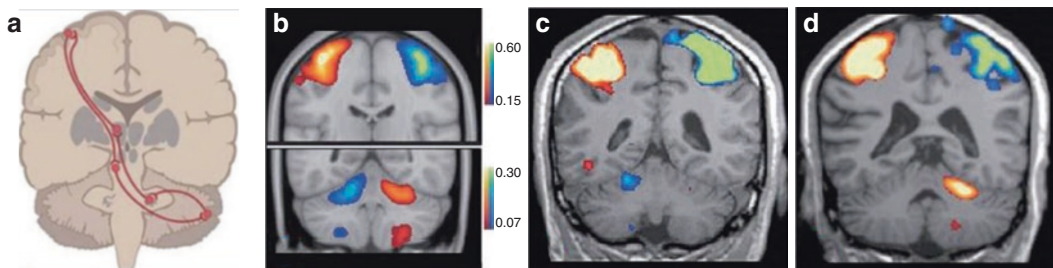


Fig. 12.16 Schematic diagram of a coronal section of the cerebro-ponto-cerebellar circuit. Main components of the cerebrocerebellar circuit. The polysynaptic efferent pathway between the cerebral cortex and the pons is mainly projected to the contralateral cerebellum. The afferent pathway is first projected to the deep cerebellar nuclei, then to the thalamus, and finally to the cerebrum (a).

Resting-state fMRI of healthy adults shows the intrinsic functional connectivity between the bilateral cerebrum and cerebellum (b). Cerebrocerebellar functional connectivity is present in patients with left (c) and right (d) pontine infarction. Functional connectivity is impaired in the affected circuit, but remains unchanged in the unaffected circuit

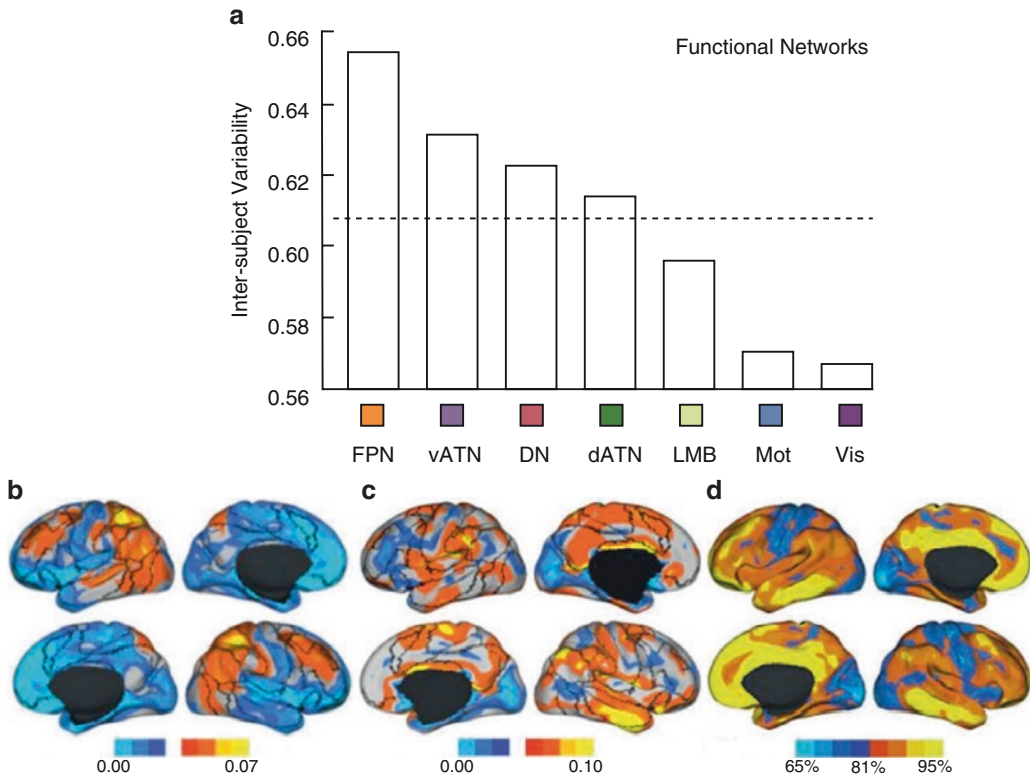


Fig. 12.17 Inter-individual variability in the functional connectivity of brain networks. Brain networks involved in higher-order cognition (control and attention network) showed greater variability, whereas the sensory, motor, and visual networks showed smaller variability (a). Brain regions that are phylogenetically the youngest (frontal

lobe, temporal lobe and parietal lobe) showed the highest variability. Inter-individual variability was correlated with sulcal depth (b), not significantly correlated with cortical thickness (c), and positively correlated with long-range connectivity (d)

Additionally, the inter-individual variability of functional connectivity was also significantly associated with behavioral differences, in that brain regions with high connectivity variability were consistent with regions of high variability in cognitive or behavioral domains as determined by behavioral studies. Taken together, these findings demonstrate that inter-individual variability in functional connectivity can characterize the different manifestations of human behavior, and therefore serve as a theoretical basis for the formulation of individualized treatment plans for patients with cerebral infarction.

With the gradual advances of resting-state fMRI technology and the continuous improvements in its data analysis methods, the multi-perspective, longitudinal evaluation of

whole-brain functional connectivity and functional networks will undoubtedly further elucidate the brain mechanisms underlying the functional reorganization after cerebral infarction, which will provide valuable information for clinical rehabilitation.

The wide range of MRI techniques have provided more options for the assessment of cerebrovascular diseases. The ability to combine histomorphological changes with data such as cerebral hemodynamics, brain metabolism, biochemical changes, white matter integrity, and functional connectivity has significant implications for attaining an in-depth understanding on the pathophysiological mechanisms underlying the pathogenesis of cerebral ischemia, and accurately evaluating the functional state of ischemic

brain tissues. Therefore, MRI continues to play a crucial role in the early diagnosis, differential diagnosis, treatment selection, dynamic lesion monitoring, efficacy evaluation, and prognostic determination of ischemic cerebrovascular disease.

12.2 Research Applications of PET Imaging in Cerebrovascular Diseases

Several ischemic cerebrovascular diseases are the result of the transient or permanent occlusion or stenosis of cerebral blood vessels, which leads to metabolic and molecular changes in brain cells, thereby causing brain dysfunction and morphological damage. The blood flow and metabolic changes of brain tissues in the ischemic core and its adjacent regions can be assessed using radionuclide imaging, especially PET, for which there are currently a variety of different tracers, such as $^{15}\text{O}\text{-H}_2\text{O}$, $^{13}\text{N}\text{-NH}_3\text{-H}_2\text{O}$, and $^{18}\text{F}\text{-fluorodeoxyglucose}$ ($^{18}\text{F}\text{-FDG}$), imaging agents for neuroinflammatory factors, imaging agents for benzodiazepine receptors, and imaging agents for hypoxia, among others. In this chapter, we have focused on the applications of PET in ischemic cerebrovascular disease and atherosclerotic plaque.

12.2.1 Applications of PET in Ischemic Cerebrovascular Diseases

12.2.1.1 Applications of PET in Acute Ischemic Cerebrovascular Diseases

CBF refers to the volume of blood passing through 100 g of brain tissue per unit of time and plays a decisive role in the maintenance of brain tissue function and metabolic levels. $^{15}\text{O}\text{-H}_2\text{O}$ PET is currently recognized as the gold standard for the quantitative measurement of CBF and is able to accurately quantify CBF values and clarify the extent of the ischemic penumbra, which is critical to facilitating early diagnosis and throm-

bolytic therapy in clinical settings. In healthy brains, the average whole-brain CBF is about 50 mL/(100 g·min), the average CBF of gray matter is higher, at 80 mL/(100 g·min), and the average CBF of white matter is about 20 mL/(100 g·min). In addition to obtaining CBF values, $^{15}\text{O}\text{-H}_2\text{O}$ PET can also be used to obtain oxygen extraction fraction (OEF) and cerebral blood metabolic rate of oxygen (CMRO₂). OEF is the percentage of oxygen taken up by a tissue after blood passes through the capillary bed, while CMRO₂ reflects the metabolic activity of brain tissues, and is a comprehensive indicator of the oxygen metabolism and utilization of the brain. Under normal physiological conditions, resting-state CBF is proportional to CMRO₂ and OEF, i.e., $\text{CMRO}_2 = \text{CBF} \times \text{OEF}$.

The conversion of cerebral ischemia to cerebral infarction is a process of dynamic change, with irreversible damage spreading from the ischemic core to the periphery. For patients with acute cerebral ischemia, the early treatment of reversible brain tissue damage is an important goal. Studies have shown that the cerebral infarct core has a CBF of <12 mL/(100 g·min) or a CMRO₂ of <65 μmol/(100 g·min). When CBF drops to 12–22 mL/(100 g·min), the ischemic region has the potential of either progressing to infarction or achieving recovery. This region is also known as the region of “misery perfusion”. Its pathophysiological mechanism involves the decrease in rCBF caused by an increased capacity for compensatory vasodilation, which implies that in order to meet their metabolic needs, neurons must extract more oxygen from inflowing blood, causing OEF to increase to as high as 80% (normal value, 40%). At this point, CBF is still higher than 22 mL/(100 g·min), however, the normal range of CBF cannot be attained due to the inadequacy of the blood supply, and this area is therefore defined as the hypoperfused region. The recovery potential of functional impairments in post-ischemic cells does not depend solely on the residual blood flow in the ischemic phase, but also on the duration of the blood flow disturbance. Preliminary PET imaging studies conducted on the duration of local ischemia in animal and human stroke models have found that PET

can be used to observe four stages of focal cerebral ischemia. The first stage is when the decrease in regional cerebral perfusion pressure (CPP) matches the decrease in the regional blood flow of cerebrovascular tissues, while the decrease in CBF induces the increase in CBV via vasodilation in order to maintain CBF stability. The second stage involves the increase in OEF as CBF decreases in order to maintain $CMRO_2$. In the third stage, the CBF and $CMRO_2$ of the infarcted brain area decrease, while OEF increases to maintain tissue metabolism as far as possible. Brain tissues in this stage are defined as the ischemic penumbra. In the fourth stage, CBF, $CMRO_2$, and OEF are all at very low levels, and brain tissues in this stage have undergone irreversible ischemic injury or infarction. A number of studies have demonstrated that determining the ischemic penumbra after stroke is the key to successful treatment and that some patients may have very a long window for effective treatment.

Brain weight accounts for only 2% of total body weight, but its oxygen consumption at rest accounts for 20% of the total basal oxygen consumption in humans, most of which is used for the oxidative metabolism of glucose. Under normal physiological conditions, glucose is the only substrate consumed in the energy metabolism of the brain. ^{18}F -FDG is the most widely used imaging agent for glucose metabolism in clinical settings. As with glucose, ^{18}F -FDG is transported into cells via glucose transporters and phosphorylated by hexokinase to form ^{18}F -FDG-6-phosphate (^{18}F -FDG-6P). However, the absence of a hydroxyl group in ^{18}F -FDG-6P prevents its further metabolism, resulting in the retention of this reaction product within the cell. Therefore, ^{18}F -FDG-6P can be used to display the distribution of glucose uptake by cells in the body. Under normal physiological conditions, neurons in cortical gray matter, basal ganglia, cerebellum, and brainstem have the greatest demand for glucose, leading to a significant elevation in ^{18}F -FDG uptake. The cerebral metabolic rate of glucose (CMRGlC) is an objective indicator that can reflect human glucose metabolism, and in a healthy human brain is approximately 25 μ mol/(100 g·min). CMRGlC is significantly correlated

with CBF, and studies have shown that when $rCBF > 40$ mL/(100 g·min), CMRGlC will remain within the normal range, but when rCBF decreases from 35 mL/(100 g·min) to 20 mL/(100 g·min), CMRGlC will undergo a sharp increase, followed by a decrease, and finally cease almost completely when $rCBF < 20$ mL/(100 g·min). Therefore, in regions with reduced CBF, this sharp increase in glucose metabolism may be of critical clinical significance and may serve as an imaging feature of the ischemic penumbra.

Although experimental stroke studies involving ^{18}F -FDG have been performed for more than 20 years, these have primarily been restricted to animal experiments, whereas clinical studies have been relatively scarce, with the majority limited to patients in the subacute phase. This may be linked, to some extent, with the long preparation process of ^{18}F -FDG and the need to wait for at least 40 min after injection before imaging can be performed. Experimental studies on ischemic stroke models in small animals and primates have demonstrated consistent trends in the reduction of ^{18}F -FDG uptake in the infarct core but found substantial spatiotemporal variations in ^{18}F -FDG uptake in the peri-infarct area. The research team led by Walberer found in a rat model of stroke that elevated ^{18}F -FDG uptake could not be observed in the peri-infarct area during the acute ischemic phase and appeared only at 1 d after onset, which was more consistent with the timing of the neuroinflammatory response. In another study, Heiss and his research team examined the PET findings of 16 patients with acute ischemic stroke at onset and during follow-up, in which the changes in the CBF, CBV, $CMRO_2$, OEF, and CMRGlC of ipsilesional and contralesional brain tissues were compared between the two time points. Their results revealed that in the infarct core, blood flow, and metabolism were significantly lower than the corresponding contralesional regions, and did not change significantly at follow-up. When the peri-infarct area was defined based on decreased $CMRO_2$, no significant changes in CBF were observed at follow-up, but there were significant reductions in $CMRO_2$, OEF, and CMRGlC, and this region was

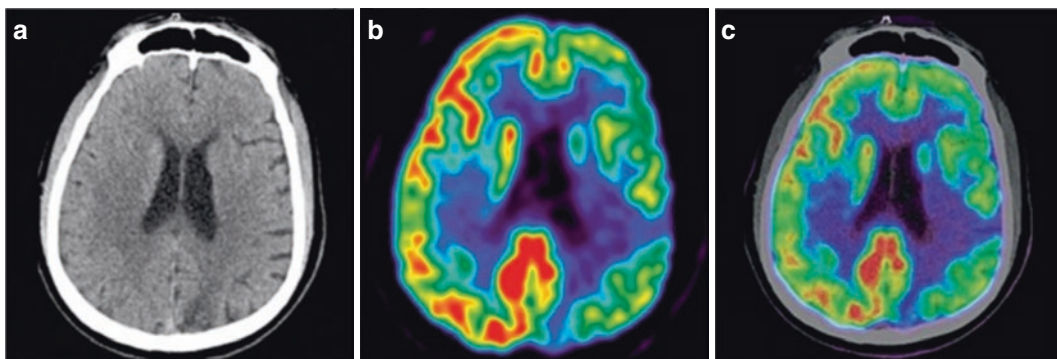


Fig. 12.18 Left intracranial artery stenosis. A 60-year-old male patient. Transverse head CT plain scan shows foliate hypodense shadows in the left parietal lobe (a). Transverse ^{18}F -FDG PET (b) and integrated ^{18}F -FDG PET/CT (c) show impaired ^{18}F -FDG uptake of the left

parietal lobe, which was 59% lower than the corresponding contralateral region; as well as reduced ^{18}F -FDG uptake in the left frontal and parietal lobes, which was 18% lower than the corresponding contralateral region

later confirmed as an infarcted area using CT. When the peri-infarct area was defined based on increased OEF, only regions with elevated OEF and slightly impaired CMRO_2 showed metabolism levels that were close to normal values (Fig. 12.18).

Hypoxia markers play an important role in the identification of ischemic tissues. Increased uptake of radiolabeled nitroimidazole derivatives can be observed in the histologically damaged ischemic core, as well as adjacent intact tissues at follow-up. ^{18}F -fluoromisonidazole (^{18}F -FMISO) is a common hypoxia marker utilized in clinical settings. Yeh et al. were the first to use ^{18}F -FMISO to examine patients with ischemic stroke and found increased ^{18}F -FMISO uptake in the peri-infarct area during the acute phase, while the decrease in this elevated uptake during the chronic stage indicated that tissues that were initially positive for ^{18}F -FMISO uptake had either been infarcted or had recovered.

12.2.1.2 Applications of PET in Chronic Cerebrovascular Diseases

Chronic ischemic cerebrovascular disease, which accounts for about 70% of all cerebrovascular disease, is largely the result of the stenosis or occlusion of the internal carotid or middle cerebral artery. In the chronic phase, CBF remains an

important metric for evaluation, but measuring CBF alone is insufficient. When CPP decreases, normal blood flow can still be maintained via the autoregulatory vasodilation of distal resistance vessels, and this autoregulatory function is known as the cerebrovascular reserve (CVR). CVR refers to the ability of distal cerebral arteries to perform compensatory dilation or constriction to maintain normal CBF under the effects of normal physiological or pathological stimuli. Clinically, resting-state, acetazolamide-challenged ^{15}O - H_2O PET is a key technique for measuring CVR. Based on the known physiological responses of CBF, CBV, and OEF to CPP reduction, researchers have proposed three stages that describe the regional cerebral hemodynamics resulting from chronic carotid occlusion. In stage 0, CPP is normal, due to the complete compensation of the occluded artery by collateral circulation; CBF and CMRO_2 are closely matched; OEF is normal; CBV is not elevated; CBF responds normally to vasodilatory stimuli; and CVR is normal. In stage I, CPP reduction is reflected in the hemodynamic impairment, and CBF is maintained via the autoregulatory vasodilation of small arteries. At this point, CBV is increased, CVR is decreased, and CBF shows a weaker response to vasodilatory stimuli, although OEF remains normal. In stage II hemodynamic failure, CPP drops below the lower limit of autoregulation, CBF decrease is

more prominent than $CMRO_2$ decrease, and CVR is reduced. At this point, OEF increases to maintain brain oxygen metabolism and tissue function, while ischemic injury may cause $CMRO_2$ to drop below the normal range. This stage is also known as “misery perfusion.” Kuroda et al. performed long-term follow-up on 77 patients with ischemic cerebrovascular disease and found that the degree of CVR impairment was better at predicting stroke risk than the degree of vascular stenosis. Therefore, the evaluation of CVR is useful for the early clinical detection of high-risk groups for stroke, enabling the implementation of early interventions.

The ^{13}N -labeled PET tracer, ^{13}N -ammonia ($^{13}N-NH_3$), is a small-molecule, neutral aqueous solution that can freely pass through the blood-brain barrier and into brain tissues with blood flow, where it is converted into glutamine and retained. Stress tests conducted using $^{13}N-NH_3 \cdot H_2O$ PET/CT have demonstrated that $^{13}N-NH_3 \cdot H_2O$ PET can reflect CVR capacity and improve the diagnostic rate of ischemic cerebrovascular disease. Researchers have combined $^{13}N-NH_3 \cdot H_2O$ with ^{18}F -FDG to study CBF and

cerebral metabolism in ischemic cerebrovascular disease. One-day integrated CBF-cerebral metabolism imaging techniques have been developed for the assessment of cerebral ischemia patients with varying extents of cerebrovascular stenosis, in order to examine the characteristics of impaired brain function. Based on qualitative and semi-quantitative analysis, CBF and metabolism were shown to match in a number of different ways, and it was therefore proposed that the joint evaluation of the two is of great value for patients with chronic ischemic cerebrovascular disease. Additionally, $^{13}N-NH_3 \cdot H_2O$ PET/CT was combined with methazolamide challenge to reflect the CVR status of patients with chronic ischemic cerebrovascular disease and evaluate their condition (Fig. 12.19).

Ischemia can cause microglial cells to switch from a quiescent to an activated state, subsequently acting as phagocytes. In this activation process, these cells may undergo morphological changes, undertake proliferation, release pro-inflammatory compounds, and increase immunomodulatory surface antigens, so as to alter their effector program. During the course of this, the

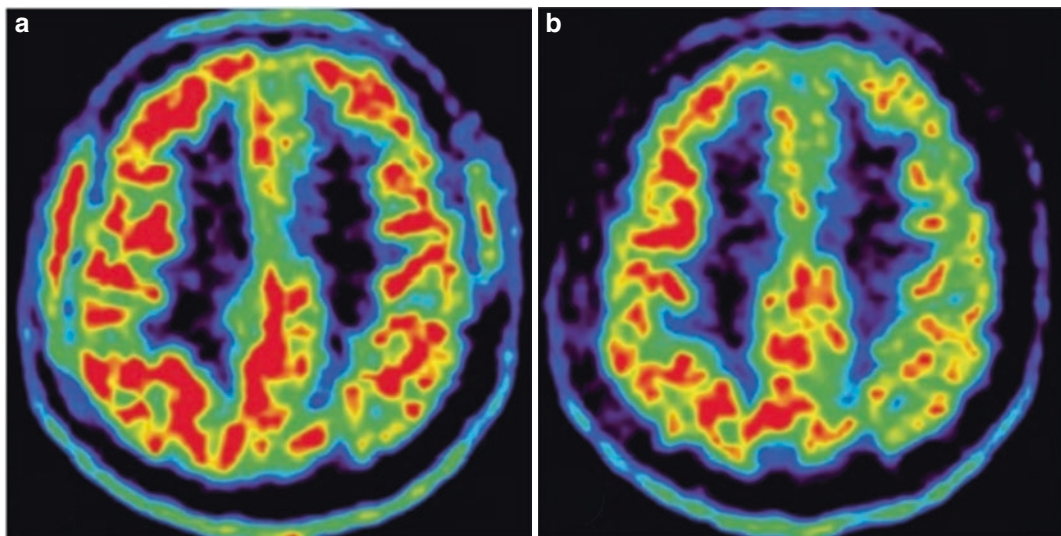


Fig. 12.19 Patient with left intracranial artery occlusion who underwent $^{13}N-NH_3 \cdot H_2O$ PET/CT with methazolamide challenge. A 50-year-old male patient. Transverse resting-state $^{13}N-NH_3 \cdot H_2O$ PET shows hypoperfusion in

the left parietal lobe (a). Transverse $^{13}N-NH_3 \cdot H_2O$ PET after methazolamide challenge shows new hypoperfused regions in the left frontal lobe in addition to the left parietal lobe (b)

translocator protein 18 kDA (TSPO), also known as benzodiazepine receptor, is upregulated on the mitochondria of activated microglial cells, and can therefore serve as an inflammatory biomarker. ^{11}C -PK11195 is a commonly used inflammatory tracer in clinical practice. Studies have observed that ^{11}C -PK11195 uptake is elevated in the ischemic core and its peripheral areas within a few days after ischemia onset.

12.2.1.3 Applications of PET in the Efficacy Evaluation of Treatments for Ischemic Cerebrovascular Disease

The prevention and treatment of ischemic cerebrovascular disease consist of medical and surgical treatments. PET imaging plays a crucial role in the preoperative assessment and prognostic determination of surgical treatment. ^{15}O - H_2O PET can accurately determine the CBF, CMRO_2 , and OEF values of brain tissues in patients with acute ischemic cerebrovascular disease. According to experimental results, CBF values less than 60% of the normal range, and CMRO_2 values greater than 40% of the normal range can be used to accurately identify the ischemic penumbra of stroke patients for intervention, thereby effectively reversing the ischemic penumbra. However, the short half-life of ^{15}O - H_2O , and therefore its need for an on-site cyclotron for production, have substantially restricted the clinical application of this technique in acute ischemic cerebrovascular disease. Surgical treatments for chronic ischemic cerebrovascular disease include endarterectomy and arterial bypass, among others, of which extracranial artery-middle cerebral artery bypass surgery is one of the most commonly utilized methods. Indications for surgery primarily include recurrent transient ischemic attacks and mild neurological impairment induced by cerebral artery stenosis or occlusion, but without symptoms such as severe hemiplegia and aphasia, perfusion imaging showing reduced CBF of the affected brain areas, and non-responsiveness to medical treatment, among others. Bypass surgery attempts to improve the patient's CBF by adding or completely replacing

the blood supply from a cerebral artery to the brain, with the goal of preventing stroke recurrence. In a prospective evaluation of 40 patients with symptomatic unilateral vascular occlusion, it was found that patients with elevated OEF had a higher risk for stroke, while the risk of recurrent stroke increased markedly with increasing OEF. Therefore, ^{15}O - H_2O PET is an important imaging technique for evaluating the therapeutic efficacy of bypass surgery. Powers et al. performed a multi-center, randomized trial involving 195 patients with symptomatic atherosclerotic internal carotid artery occlusion to investigate the therapeutic efficacy of medical and surgical treatments. Their results demonstrated that OEF values as measured by ^{15}O - H_2O PET were crucial in identifying patients at high risk for recurrent stroke due to poor collateral circulation. They also found that compared with medical treatment alone, bypass surgery plus medical treatment did not reduce the risk of recurrent ipsilateral ischemic stroke within 2 years. However, this study has been criticized for its poor design and implementation, and therefore, further investigations are currently ongoing concerning the evaluation of specific indications for bypass surgery.

^{18}F -FDG PET has also been utilized to evaluate the efficacy of surgical and interventional treatments for chronic ischemic cerebrovascular disease. An ^{18}F -FDG PET study on 19 patients with chronic carotid artery stenosis or occlusion found that carotid artery stent placement led to improvements in postoperative cerebral glucose metabolism and neurocognitive function. The research team led by Yu performed pre- and post-operative imaging assessments on patients with chronic cerebral ischemia undergoing bypass surgery. Their results indicated that ipsilesional CBF and ^{18}F -FDG uptake were both higher than preoperative levels, and patients experienced improvements in all symptoms within 1 month after surgery. Furthermore, surgery can help to increase the CBF and ^{18}F -FDG uptake of regions with hypoperfusion and reduced ^{18}F -FDG uptake. However, in-depth studies have not been conducted on the long-term changes in cerebral metabolic levels.

12.2.2 Applications of PET in Atherosclerotic Plaque

Carotid atherosclerosis is currently the primary cause of ischemic stroke in China, with about 70% of ischemic strokes resulting from the rupture of carotid atherosclerotic plaques. Therefore, the early identification of vulnerable plaques and the evaluation of plaque stability are of utmost importance in preventing and controlling the onset of ischemic stroke events. Atherosclerosis is a systemic, chronic, inflammatory disease of the vessel walls caused by vascular risk factors that can gradually progress into vulnerable plaques, and eventually result in the occurrence of cerebrovascular events. Studies have shown that vulnerable plaques can rupture to form emboli that enter the bloodstream and cause thromboembolisms, which in turn can lead to ischemic stroke. Intraplaque neovascularization and macrophage inflammation are key factors contributing to the vulnerability of carotid plaques. Plaque vulnerability is determined by plaque composition, while the different stages in plaque progression are characterized by different inflammatory responses. Common characteristics of vulnerable plaques include a large lipid-rich necrotic core with a thin overlying fibrous cap, containing abundant macrophages, T lymphocytes, and some smooth muscle cells.

Morphological imaging has certain drawbacks in the diagnosis of vulnerable carotid plaques. Therefore, molecular imaging techniques, especially molecular probes for nuclear imaging, have now become a hotspot of research in this field. Every step in the pathophysiological mechanism underlying the onset of carotid plaques and their development into vulnerable plaques is an important target for molecular imaging. The primary processes include inflammatory cell aggregation, endothelial cell activation, macrophage apoptosis, intraplaque hypoxia, neovascularization and subsequent microcalcification, fibrous cap degradation, and thrombosis, which ultimately lead to ischemic stroke onset. PET is a common molecular imaging technique that involves the specific radiolabeling of molecular tracers to achieve the visual, non-invasive analysis of *in vivo* cellular metabolic activity. At pres-

ent, a wide range of molecular imaging methods have been established for tumor imaging, and have been utilized to clarify the molecular mechanisms of tumorigenesis. Owing to the similarities in molecular imaging targets, these techniques can also be applied to carotid atherosclerotic plaques. However, due to the poor resolution of PET imaging, it is essentially unable to discriminate among the various anatomical features. Therefore, many multimodal imaging techniques have emerged recently, and the application of PET/CT and PET/MR techniques has gradually enhanced the specificity and sensitivity of PET scans. The combination of PET with CT or MRI can be used to identify the components of atherosclerotic plaques and the degree of inflammatory response, which allows us to accurately assess the vulnerability of carotid plaques.

12.2.2.1 Applications of ^{18}F -FDG PET in Carotid Atherosclerotic Plaque

^{18}F -FDG is currently the most widely used molecular imaging tracer for the evaluation of plaque inflammation. ^{18}F -FDG is phosphorylated by hexokinase to form ^{18}F -FDG-6P, which cannot undergo further glycolysis due to its lack of a hydroxyl group, and is therefore retained intracellularly, while its retention is especially prominent in metabolically active inflammatory cells, such as intraplaque activated macrophages. This, therefore, is the basis for the ^{18}F -FDG PET molecular imaging of inflammatory vulnerable carotid plaques. In animal models and clinical studies, ^{18}F -FDG uptake was found to be closely associated with macrophage aggregation. Hyafil et al. showed that the lipid-rich necrotic core of non-stenotic carotid plaques as detected by MRI was significantly associated with high ^{18}F -FDG uptake. Tawakol et al. demonstrated that ^{18}F -FDG PET can be used to evaluate the inflammatory activity of plaques after drug therapy. Therefore, ^{18}F -FDG PET can monitor the degree of inflammatory response in vulnerable plaques, and hence predict the risk of ischemic stroke onset, which facilitates the clinical risk stratification of stroke onset among patients with carotid atherosclerosis, and the formulation of individualized treatment plans.

A study involving patients with recently symptomatic carotid stenosis found that ^{18}F -FDG uptake related to intraplaque inflammation was associated with the risk of early stroke recurrence. Furthermore, ^{18}F -FDG PET studies have revealed significant differences in the target-to-background ratio (TBR) between symptomatic and asymptomatic plaques, as well as between plaques positive and negative for microembolic signals. Therefore, ^{18}F -FDG PET can accurately detect high-risk carotid plaques, and predict the risk of atherosclerosis progression and thrombotic complications.

12.2.2.2 Applications of Other PET Tracers in Vulnerable Carotid Plaques

In addition to ^{18}F -FDG, a number of other tracers can also be utilized in the imaging of carotid plaques, so as to determine their level of vulnerability. These include tracers specific to the occurrence of hypoxia, neovascularization, and microcalcification in the pathological process of plaque formation, as well as novel PET tracers for atherosclerosis.

1. Other PET tracers based on the plaque formation process:

- (a) ^{18}F -FMISO: The lack of normal blood vessels in carotid atherosclerotic plaques often gives rise to hypoxia, while hypoxia is closely related to plaque volume and plaque inflammation. ^{18}F -FMISO PET has been extensively utilized in the imaging of hypoxic atherosclerosis. Researchers have demonstrated using a rabbit model of hyperlipidemia that ^{18}F -FMISO uptake is significantly elevated in atherosclerotic areas. Studies have also shown that ^{18}F -FMISO PET allows the visual analysis of hypoxic regions in atherosclerosis.
- (b) ^{68}Ga -NOTA-RGD: Neovascularization frequently occurs within vulnerable carotid plaques. Over the course of plaque progression, new blood vessels are prone to rupture and hemorrhage, which causes thromboembolism, and eventually leads to the occurrence of ischemic stroke. ^{68}Ga -NOTA-RGD targets integrin $\alpha v \beta 3$

which is specifically expressed on the surface of vascular endothelial cells and macrophages. Therefore, PET/CT imaging performed on mouse models of atherosclerosis and patients' blood vessels enables the visual assessment of atherosclerosis.

- (c) ^{18}F -sodium fluoride (^{18}F -NaF): Calcification is the final outcome of inflammation, and one of the key features of atherosclerosis. Microcalcification primarily occurs in the fibrous cap overlying the plaque surface, and contributes significantly to plaque vulnerability. ^{18}F -NaF is a specific tracer commonly used to detect bone metastases. Studies have shown that ^{18}F -NaF can be taken up by atherosclerotic vessel walls, and is associated with the risk factors of atherosclerosis. Other studies have found that ^{18}F -NaF uptake is significantly higher in vulnerable carotid plaques than in contralateral asymptomatic plaques and the control group. The study by Li et al. demonstrated that ^{18}F -NaF PET/CT was useful in the detection of microcalcification activity in carotid atherosclerosis, and can assess the stability of carotid plaques, while low-dose CT can help to determine the degree of plaque calcification and plaque localization (Fig. 12.20).
- #### 2. Novel PET tracers:
- (a) $^{99\text{m}}\text{Tc}$ -HYNIC-IL-2: Interleukin 2 (IL-2) and scavenger receptors are expressed on the surface of macrophages. $^{99\text{m}}\text{Tc}$ -HYNIC-IL-2 is a biological probe targeting IL-2 and has been widely utilized in the imaging of carotid plaques.
 - (b) ^{64}Cu -DOTA-DAPTA: As an effective molecular probe for carotid atherosclerosis, this compound has a strong affinity for various chemokine receptors.
 - (c) ^{68}Ga -DOTA-TATE: This compound has a specific affinity for type II somatostatin (SST) receptor, which is overexpressed in activated macrophages and injured endothelial cells. Studies have shown that atherosclerotic vessels exhibited a significant

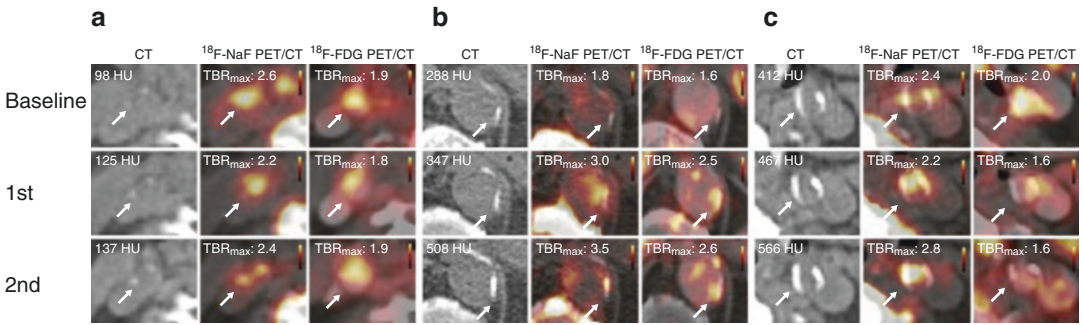


Fig. 12.20 Comparative study of ¹⁸F-FDG PET/CT and ¹⁸F-NaF PET/CT in carotid atherosclerosis progression. Transverse ¹⁸F-NaF-PET/CT scan of myeloma patients with varying degrees of carotid artery calcification. In non-calcified lesions, the location of ¹⁸F-NaF uptake in the carotid plaque was consistent with that of ¹⁸F-FDG, and

both showing increased calcium uptake (a). In mildly calcified lesions, after progressive arterial calcium accumulation, ¹⁸F-NaF uptake showed significant increases from baseline to follow-up (b). In severely calcified lesions, dense calcium components can be observed (c). Arrows indicate calcified lesions

correlation between ⁶⁸Ga-DOTA-TATE and ¹⁸F-FDG uptake.

- (d) ¹⁸F-FMCH: Cho plays an important role in the process of cell membrane formation. Studies on atherosclerotic plaques in mice found that tracing with ¹⁸F-FMCH (targeting macrophage cell membrane receptors) and ¹¹C-Cho enhanced the detection of macrophages in the inflammatory response.
- (e) ¹¹C-PK11195: TSPO is widely found in the outer mitochondrial membrane and expressed in some macrophages. Gaemperli et al. performed ¹¹C-PK11195 (targeting TSPO) PET/CT imaging in carotid plaques and found that this technique significantly increased the detection of vulnerable carotid plaques.
- (f) ^{99m}Tc-RP805: During proteolysis, macrophages produce a variety of proteases, of which matrix metalloproteinase (MMP) is the most common and can be specifically tagged using the ^{99m}Tc-RP805 tracer. Studies have demonstrated that this tracer can be used for plaque imaging in animal models.
- (g) ^{99m}Tc-cAbVCAM1-5: Endothelial cells are activated during the inflammatory response of atherosclerosis, while the vascular cell adhesion molecule 1 (VCAM-1) found on their cell surface can serve as a target for tracers. Studies have shown that PET imaging of vulner-

able plaques in mouse models could be carried out effectively using ⁶⁴Cu-P-selectin monoclonal antibody ($T_{1/2} = 12.7$ h) and ^{99m}Tc-cAbVCAM1-5.

- (h) ⁶⁸Ga-pentixafor: This compound can trace the type 4 chemokine receptor (CXCR4) found on macrophages involved in atherosclerosis progression. Kircher et al. performed a retrospective analysis on 92 patients with atherosclerosis who underwent ⁶⁸Ga-pentixafor PET/CT and ¹⁸F-FDG PET/CT imaging. They found that ⁶⁸Ga-pentixafor PET/CT identified more atherosclerotic plaques than ¹⁸F-FDG PET/CT, and the two showed a weak correlation. Therefore, their findings demonstrate that ⁶⁸Ga-pentixafor could serve as a useful tracer for the evaluation of vulnerable atherosclerotic plaques.

PET is a valuable molecular imaging technique for the quantification of CBF and metabolism, which allows the accurate evaluation of CVR function through its intrinsic connections and dynamic evolution. Therefore, this technique can provide objective imaging evidence for the risk stratification of patients with cerebral ischemia, thereby achieving the early warning of cerebral infarction as well as the individualized and precise diagnosis and treatment of patients, which effectively reduces the incidence rate of cerebral infarction.

12.3 Research Applications of PET/MR in Cerebrovascular Diseases

MRI is commonly utilized for the examination of cerebrovascular diseases, as it provides detailed anatomical images as well as information on brain function, perfusion, tissue biochemical changes, and other characteristics. PET is also an important tool in the study of neurological diseases, while the development and application of a wide variety of specific tracers have played a crucial role in studying the pathogenic mechanisms of cerebrovascular diseases, as well as guiding its early diagnosis and treatment. Integrated PET/MR combines PET molecular imaging techniques with multiparametric MRI techniques for the acquisition of comprehensive imaging information in a single scan session. This approach not only allows the visualization of metabolic levels in brain tissue lesions, but also the precise anatomical location, hemodynamic changes, diffusion characteristics, and biochemical information of these lesions. Therefore, PET/MR can provide a strong support for further investigating the pathophysiological mechanisms of ischemic cerebrovascular disease, elucidating the trends in its pathogenesis, and guiding individualized clinical treatment.

12.3.1 Applications of Integrated PET/MR in Cerebrovascular Diseases

12.3.1.1 Applications of Non-invasive Quantitative Methods with Integrated PET/MR

Integrated PET/MR not only enables the precise co-registration of PET and MRI data, but also allows the simultaneous acquisition of information on CBF, cerebral metabolism, brain functional network connectivity, and white matter fiber bundles. There is currently an urgent clinical need to further understand the pathophysiological mechanisms of ischemic cerebrovascular disease. CBF is one of the key quantitative indicators of ischemic cerebrovascular disease. As mentioned previously, the gold standard for the

quantification of CBF is $^{15}\text{O}\text{-H}_2\text{O}$ PET, the traditional method of which involves administering a bolus of $^{15}\text{O}\text{-H}_2\text{O}$, and tracking the dynamic processes as the tracer reaches the brain, while also sampling arterial blood from the radial artery at different time points during the acquisition process. Then, using arterial blood as the input function, image processing is performed to obtain a time-radioactivity curve of specified brain areas, in order to calculate the CBF values. However, this method requires the sampling of arterial blood, which has restricted its widespread application in clinical settings. Su et al. proposed an image-derived arterial input function (IDAIF) method of CBF quantification involving the co-registration of PET and MRA images acquired using separate scanners. In their study, 8 healthy volunteers underwent either the conventional arterial sampling method or the IDAIF method for the calculation of whole-brain CBF, and the correlation between the two methods was examined. Their results revealed that the CBF calculated using these two methods were highly correlated ($r = 0.93$), implying that the IDAIF method could replace the conventional arterial sampling method for the calculation of CBF. Integrated PET/MR offers the unique advantage of simultaneous scanning, allowing both PET and MRI data to be acquired at the same time in a single scan session. Therefore, the precise co-registration between the two sets of images enables the easy and accurate acquisition of IDAIF information, and as such is more suitable for the non-invasive and absolute quantitative research on CBF.

In 2017, the same research team built upon their previous study involving separate scanners and performed integrated PET/MR on 7 healthy volunteers to compare the calculation results between the arterial sampling and IDAIF methods. The CBF calculated using the two methods showed strong agreement ($r = 0.88$), and the difference between them was not statistically significant. In current clinical settings, ASL and PWI are often used to replace $^{15}\text{O}\text{-H}_2\text{O}$ PET for the quantitative measurement of CBF. Zaro et al. used the ischemic regions delineated by $^{15}\text{O}\text{-H}_2\text{O}$ PET to guide the selection of PWI maps. Their results indicated that PWI achieved the highest accuracy at predicting the CBF critical flow

threshold when time-to-maximum (T_{\max}) > 6.1 s and TTP > 4.8 s. Therefore, the integration of $^{15}\text{O}\text{-H}_2\text{O}$ PET and PWI to evaluate the differences in perfusion as displayed by PWI and PET can help to address the current bottleneck in the development of perfusion imaging in acute ischemic stroke and has significant implications for further elucidating the pathophysiological changes in this disease. ASL is a non-invasive MRI technique that can also provide quantitative rCBF images. Using integrated PET/MR, Okazawa et al. performed a quantitative comparison of $^{15}\text{O}\text{-H}_2\text{O}$ PET and ASL in 11 healthy volunteers, which revealed that the quantitative results from ASL were slightly higher than those of $^{15}\text{O}\text{-H}_2\text{O}$ PET, and compared the differences between the two techniques can help to guide the clinical application of ASL. Additionally, Puig et al. performed integrated PET/MR on 14 healthy volunteers, in order to perform a quantitative comparison of ASL and $^{15}\text{O}\text{-H}_2\text{O}$ PET perfusion parameters in the resting state, during hyperventilation, and after acetazolamide use. No significant differences in CBF values were found between the two techniques in any state.

12.3.1.2 Evaluation of Chronic Ischemic Cerebrovascular Disease with Integrated PET/ MR

PET studies have found that some patients with ischemic cerebrovascular disease exhibit crossed cerebellar diaschisis (CCD), in which supratentorial brain lesions result in reduced blood flow and metabolism of the contralateral cerebellum. This phenomenon was first reported by Baron et al. in 1980. They utilized non-invasive $^{15}\text{O}\text{-H}_2\text{O}$ PET imaging to reveal the decreases in blood flow and oxygen metabolic rates of the contralesional cerebellar hemisphere in patients with supratentorial brain infarction. Researchers have subsequently utilized other techniques, such as CMRO_2 and CMRGlc , to further investigate this phenomenon, and confirmed the existence of CCD. The occurrence of CCD may be the result of pathologies in the cortico-ponto-cerebellar pathway and can appear immediately after the onset of ischemic stroke. This phenomenon, however, can be

reversed with successful reperfusion therapy. The occurrence of CCD is closely related to the inadequate perfusion of the frontal lobe and thalamus. fMRI studies have demonstrated the presence of CCD in patients with acute, subacute, and chronic ischemic cerebrovascular disease, while the severity of CCD in subacute patients was associated with their neurological severity and clinical outcomes. Researchers at the University of Zurich found that among patients with ischemic cerebrovascular disease, the detection of CCD using BOLD fMRI with a carbon dioxide challenge demonstrated a similar sensitivity compared to acetazolamide-challenged $^{15}\text{O}\text{-H}_2\text{O}$ PET. In the study by Kim et al. on patients with CCD after cerebral infarction, PET imaging showed reduced metabolism in the contralateral cerebellum, while DTI also revealed significantly lower FA values in the contralesional middle cerebellar peduncle, signifying the presence of damage to the cortico-ponto-cerebellar pathway. Nevertheless, the specific mechanisms underlying the onset of CCD are poorly understood, while findings on the impairments and dynamic changes of functional connectivity and fiber bundles in CCD, as well as their relationship with CBF and metabolic changes, remain inconclusive. Furthermore, this phenomenon can occur in both acute and chronic ischemia, while similar effects have also been observed in non-ischemic lesions such as brain tumors.

Brain perfusion and metabolism are both inextricably linked with neural activity and are therefore crucial physiological indicators of the state of brain function. Due to the extremely high energy demand of nervous tissues, the oxidative metabolism of glucose is virtually the only substrate for brain energy metabolism under normal physiological conditions. The glucose metabolized within neurons is primarily used to support cellular nutrition and maintain cellular functions. Generally speaking, the energy consumed by signal conduction, such as the propagation of action potentials and postsynaptic ion channels, accounts for 87% of total energy consumption, while the remaining 13% is used to maintain the resting membrane potential of neurons. Research has shown that blood flow is highly correlated

with metabolism and that this correlation decreases with increasing age. Among patients with chronic ischemic cerebrovascular disease, the early, comprehensive, and meticulous assessment of brain function, as well as the timely intervention in high-risk groups, can facilitate the prevention of stroke recurrence. In a study previously conducted by the authors, we found that performing simultaneous ^{18}F -FDG PET and ASL on patients with chronic ischemic cerebrovascular disease who required bypass surgery reflected the patient's preoperative hemodynamic and metabolic status in the non-infarcted area. After surgery, significant increases were observed in the

blood flow and metabolism of ipsilesional brain areas, and patients experience marked improvement in symptoms. Therefore, this technique is essential for the prevention of stroke recurrence and the evaluation of surgical efficacy (Fig. 12.21). Additionally, we have also analyzed the combination of ^{18}F -FDG PET and DWI when utilized in the evaluation of chronic ischemic cerebrovascular disease, which revealed reduced ^{18}F -FDG uptake in the infarct core, whereas peri-infarct tissue that appeared normal in structural MRI showed reduced ^{18}F -FDG uptake and elevated ADC values. These findings may have been due to ischemia-induced microcirculatory dys-

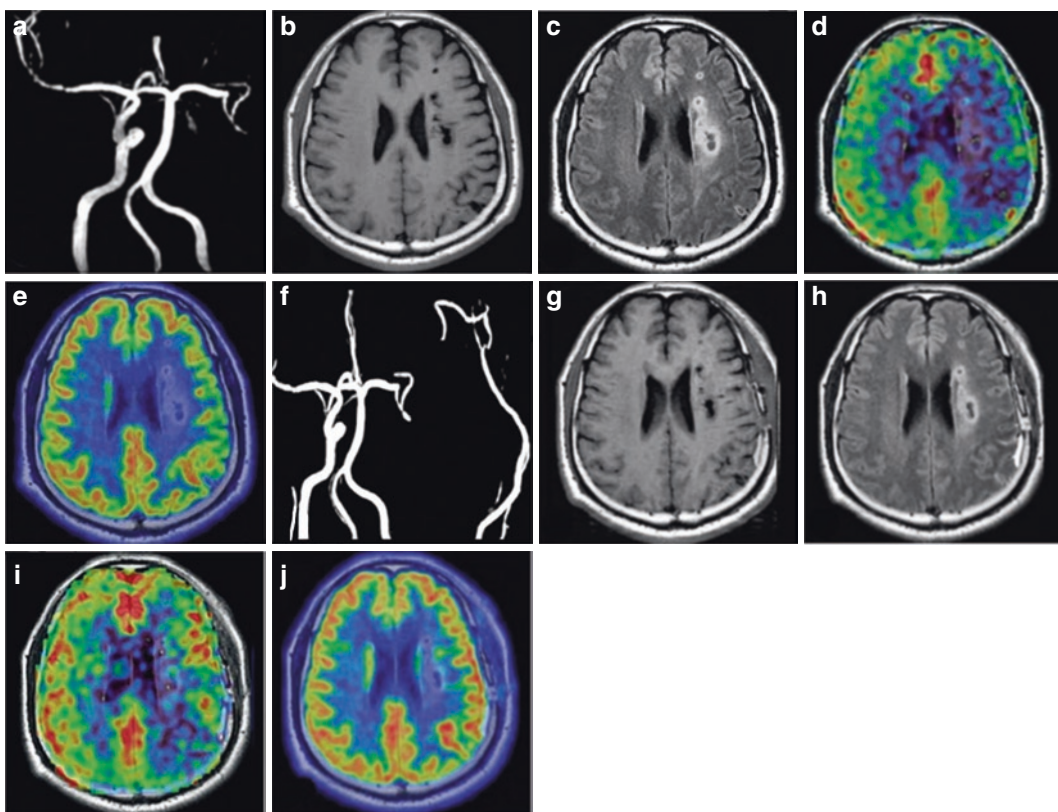


Fig. 12.21 Left internal carotid artery occlusion treated with bypass surgery. A 45-year-old male patient who presented with restricted movement of the right limbs for 7 months. Preoperative images of bypass surgery. MRA shows left carotid artery occlusion (a). MRI shows infarcts in the left corona radiata, manifesting as T₁WI hypointensities (b), and FLAIR hyperintensities (c). Integrated ASL-MRI shows decreased CBF (d), which was approximately 30 mL/(100 g·min). ^{18}F -FDG PET/MR shows

reduced ^{18}F -FDG uptake (e), and a mean standardized uptake value (SUV_{mean}) of about 7.51. Postoperative images of bypass surgery. MRA shows the left bypass graft (f). MRI with T₁WI (g) and FLAIR (h) reveals the same left corona radiata infarcts as in preoperative imaging. Increases can be observed in the CBF measured by ASL-MRI (i) and cerebral metabolism measured by ^{18}F -FDG PET/MR (j), showing a CBF of about 50 mL/(100 g·min) and SUV_{mean} of about 8.0

function, which led to increased cellular permeability, increased extracellular water, and other factors. However, further investigation is needed to elucidate the exact mechanisms involved in this process.

12.3.2 Applications of Integrated PET/MR in Carotid Atherosclerotic Plaque

PET/MR is currently the most advanced imaging technique available that can implement the simultaneous acquisition of MRI and ^{18}F -FDG PET data in a single session, and can therefore achieve the precision co-registration of the two sets of images. Additionally, this technique can also provide information on the inflammatory response of carotid atherosclerotic plaques at the morphological and molecular levels, which permits the real-time fusion of anatomical, functional, and metabolic information, thereby more accurately evaluating the stability of carotid plaques. Furthermore, MRI has obvious advantages over PET/CT, including its lack of radiation and ability to achieve high-resolution imaging of soft tissues, allowing carotid atherosclerotic plaques to be displayed more clearly.

12.3.2.1 Research Applications of ^{18}F -FDG in Carotid Atherosclerotic Plaque

^{18}F -FDG is the most common PET tracer used in clinical settings, and studies have demonstrated the benefit of performing ^{18}F -FDG PET/MR to evaluate the stability of atherosclerotic plaques. Li et al. compared the value of ^{18}F -FDG PET/MR and ^{18}F -FDG PET/CT in the evaluation of carotid plaques, and found no significant differences in PET findings between the two hybrid systems in the case of vein bypass surgery, whereas the errors resulting from different attenuation correction algorithms used could be ignored. Therefore, these findings are a direct reflection of the reliability of the PET/MR system, while the higher soft tissue contrast and multiple sequences of high-resolution MRI could better display the structure of the carotid artery wall than CT

(Fig. 12.22). Ripa et al. performed ^{18}F -FDG PET/MR and ^{18}F -FDG/CT on the carotid arteries of six male patients positive for the human immunodeficiency virus (HIV), and found significant correlations in the mean standardized uptake value (SUV_{mean}) and maximum SUV (SUV_{max}) between the two imaging techniques (SUV_{mean} : $r = 0.98$; SUV_{max} : $r = 1.00$; both: $P < 0.001$). Therefore, they concluded that ^{18}F -FDG PET/MR can effectively be used to evaluate the stability of carotid atherosclerotic plaques. Mootaz et al. performed ^{18}F -FDG PET/MR on seven patients with carotid plaques, who were divided according to scan times into standard and low dose groups. They found that the standard ^{18}F -FDG dose in ^{18}F -FDG PET/MR scans could be reduced by 75% while still ensuring high image quality and precise quantification. The results of the study by Rischpler et al. demonstrated that after the administration of drug therapy in patients with carotid atherosclerotic plaques, ^{18}F -FDG PET/MR could detect the metabolic changes of inflammatory cells in carotid plaques, and was therefore useful for determining the efficacy of clinical drug therapies.

12.3.2.2 Research Applications of Other Tracers in Carotid Atherosclerotic Plaque

In addition to ^{18}F -FDG, the utilization of other novel tracers can enhance the accuracy and specificity of PET/MR in evaluating the stability of carotid plaques. ^{68}Ga -pentixafor can trace CXCR4 in macrophages over the course of atherosclerosis progression, which has significant implications in the quantitative evaluation of the stability of carotid atherosclerotic plaques. Li et al. performed ^{68}Ga -pentixafor PET/MR on the atherosclerotic lesions of 38 tumor patients, and their TBR values were calculated. Their results indicated that the TBR value of the descending aorta wall was significantly higher in men than in women [(1.9 \pm 0.3) vs. (1.7 \pm 0.2), respectively; $P < 0.05$], and that compared with patients with a mean TBR ≤ 1.70 , those with a mean TBR > 1.70 had significantly higher incidence rates of diabetes, hypertension, hypercholesterolemia, and cardiovascular disease. Furthermore,

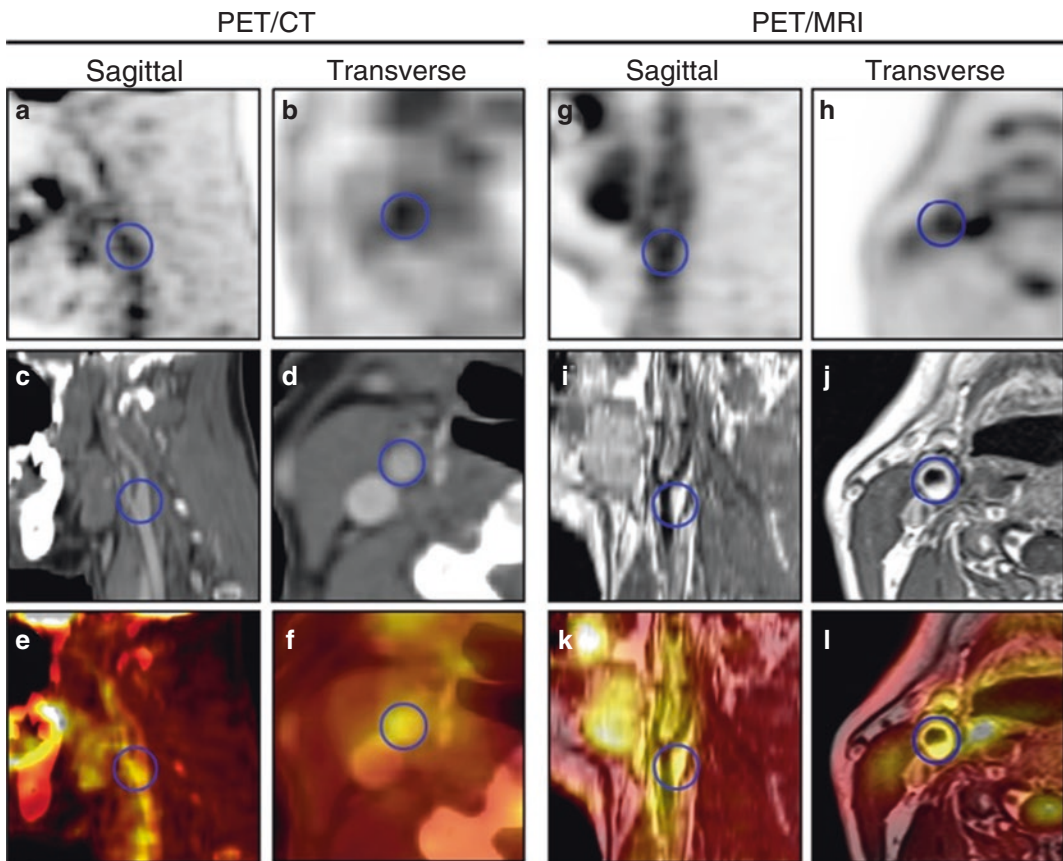


Fig. 12.22 Integrated PET/CT and MR images of the right carotid artery in a patient with head and neck cancer. A 52-year-old male patient whose right carotid plaque

shows focal ^{18}F -FDG uptake (the blue circle indicates the plaque at the carotid bifurcation)

^{68}Ga -pentixafor uptake has good reproducibility ($r = 0.60$, $P < 0.01$), and studies have shown that patients with high ^{68}Ga -pentixafor uptake have an elevated incidence of cardiovascular risk factors. Therefore, ^{68}Ga -pentixafor PET/MR is a powerful imaging technique that can be utilized to evaluate the stability of atherosclerotic plaques.

Subsequently, Li et al. performed ^{68}Ga -pentixafor PET/MR on 72 patients with lymphoma to examine carotid plaques with various lesions and confirmed through histopathology and immunohistochemistry analyses that the CXCR4 expression of atherosclerotic plaques can serve as a surrogate marker for inflammatory atherosclerosis. They concluded, therefore, that ^{68}Ga -pentixafor PET/MR can quantify the

CXCR4 expression of atherosclerotic plaques to assess plaque stability (Fig. 12.23).

The rupture of carotid atherosclerotic plaques is a major cause of ischemic stroke and represents a serious threat to human health. Therefore, the early identification of vulnerable plaques, along with the evaluation of plaque stability, is critical for achieving early clinical intervention. High-resolution MRI can accurately provide morphological information on plaque composition but cannot accurately assess intraplaque inflammation. In contrast, PET can quantify intraplaque macrophage-mediated inflammation but has a relatively poor spatial and tissue resolution. Therefore, combining PET with high-resolution MRI allows us to accurately assess the vulnerability

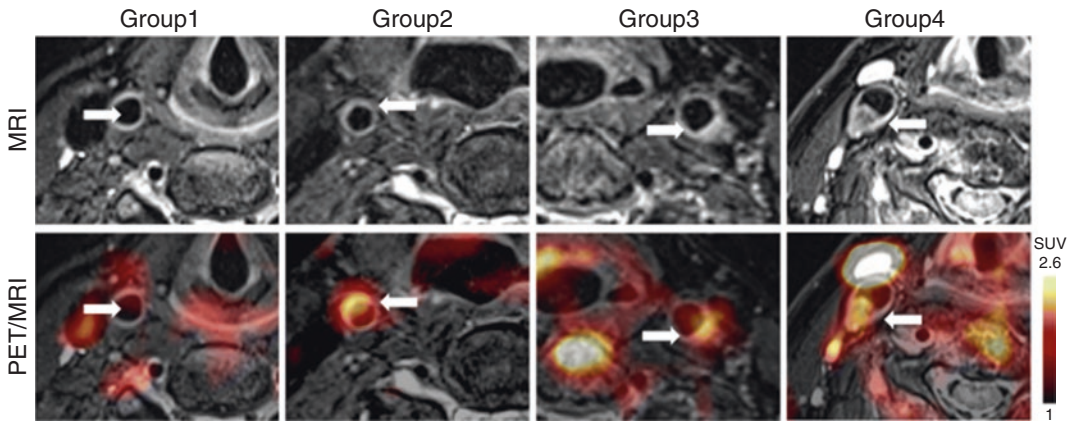


Fig. 12.23 ^{68}Ga -pentixafor PET/MR of carotid plaques with different lesions. Transverse MRI of carotid artery (a). Transverse integrated PET/MR of carotid artery (b). Focal ^{68}Ga -pentixafor uptake can be observed in a mildly atherosclerotic carotid artery with slightly eccentric thick-

ening. Significant ^{68}Ga -pentixafor can be observed in a moderately atherosclerotic carotid artery with significant eccentric thickening. No increased uptake is observed in a non-significantly eccentric control carotid artery (arrows indicate arterial regions of interest)

of carotid plaques. Integrated PET/MR allows the simultaneous acquisition of MRI and PET within a single scan session, ensuring the precise co-registration between the two sets of images. Therefore, it can be utilized for the qualitative and quantitative analysis of carotid intraplaque inflammation, while also providing information on plaque morphological structure and inflammatory cell metabolism, thereby achieving a more accurate assessment of plaque stability. This technique, therefore, holds great value for the early warning and effective prevention of ischemic stroke in clinical practice.

Suggested Reading

- Baskin A, Buchegger F, Seimille Y, et al. PET molecular imaging of hypoxia in ischemic stroke: an update. *Curr Vasc Pharmacol.* 2015;13(2):209–17.
- Calcagno C, Ramachandran S, Izquierdo-Garcia D, et al. The complementary roles of dynamic contrast-enhanced MRI and ^{18}F -fluorodeoxyglucose PET/CT for imaging of carotid atherosclerosis. *Eur J Nucl Med Mol Imaging.* 2013;40(12):1884–93.
- Carter AR, Astafiev SV, Lang CE, et al. Resting inter-hemispheric functional magnetic resonance imaging connectivity predicts performance after stroke. *Ann Neurol.* 2010;67(3):365–75.
- Cui C, Cui C, Ma Y, et al. Characteristics of cerebral blood flow and glucose metabolism in patients with different severities of cerebrovascular stenosis evaluated by one-day PET cerebral blood flow and metabolism combined imaging. *J Clin Exp Med.* 2020;19(4):427–30.
- Cui C, Ma Y, Wang M, et al. Preliminary research on the impairment characteristics of cerebral metabolism and blood flow in patients with severe cerebrovascular stenosis. *Int J Radiat Med Nucl Med.* 2014;3:141–7.
- Cui B, Zhang T, Ma Y, et al. Simultaneous PET-MRI imaging of cerebral blood flow and glucose metabolism in the symptomatic unilateral internal carotid artery/middle cerebral artery steno-occlusive disease. *Eur J Nucl Med Mol Imaging.* 2019a;47(7):1668–77.
- Cui B, Zhang M, Ma J, et al. Integrated ^{18}F -FDG PET/MRI evaluation of ischemic cerebrovascular disease. *Chin J Med Imaging Tech.* 2019b;35(12):1817–22.
- Evans NR, Tarkin JM, Buscombe JR, et al. PET imaging of the neurovascular interface in cerebrovascular disease. *Nat Rev Neurol.* 2017;13(11):676–88.
- Golestani AM, Tymchuk S, Demchuk A, et al. Longitudinal evaluation of resting-state fMRI after acute stroke with hemiparesis. *Neurorehabil Neural Repair.* 2013;27(2):153–63.
- Heiss WD. Radionuclide imaging in ischemic stroke. *J Nucl Med.* 2014;55(11):1831–41.
- Heiss W, Zaro WO. Validation of MRI determination of the penumbra by PET measurements in ischemic stroke. *J Nucl Med.* 2017;58(2):187–93.
- Hyafil F, Schindler A, Sepp D, et al. High-risk plaque features can be detected in non-stenotic carotid plaques of patients with ischaemic stroke classified as cryptogenic using combined ^{18}F -FDG PET/MR imaging. *Eur J Nucl Med Mol I.* 2016;43(2):270–9.

- Kao H, Lin M, Wu W, et al. Improvement of cerebral glucose metabolism in symptomatic patients with carotid artery stenosis after stenting. *Clin Nucl Med*. 2015;40(9):701–7.
- Kircher M, Tran-Gia J, Kemmer L, et al. Imaging inflammation in atherosclerosis with CXCR4-directed ⁶⁸Ga-pentixafor PET/CT: correlation with ¹⁸F-FDG PET/CT. *J Nucl Med*. 2020;61(5):751–6.
- Li X, Heber D, Gonzalez JC, et al. Association between osteogenesis and inflammation during the progression of calcified plaque evaluated by ¹⁸F-Fluoride and ¹⁸F-FDG. *J Nucl Med*. 2017;58(6):968–74.
- Li X, Heber D, Rausch I, et al. Quantitative assessment of atherosclerotic plaques on ¹⁸F-FDG PET/MRI: comparison with a PET/CT hybrid system. *Eur J Nucl Med Mol Imaging*. 2016;43(8):1503–12.
- Li X, Yu W, Wollenweber T, et al. ⁶⁸Ga-pentixafor PET/MR imaging of chemokine receptor 4 expression in the human carotid artery. *Eur J Nucl Med Mol Imaging*. 2019;46(8):1616–25.
- Lu J, Liu H, Zhang M, et al. Focal pontine lesions provide evidence that intrinsic functional connectivity reflects polysynaptic anatomical pathways. *J Neurosci*. 2011;31(42):15065–71.
- Lyu JH, Ma N, Liebeskind D, et al. Arterial spin labeling MRI estimation of antegrade and collateral flow in unilateral middle cerebral artery stenosis. *Stroke*. 2016;47(2):428–33.
- Mateo J, Izquierdo-Garcia D, Badimon J, et al. Noninvasive assessment of hypoxia in rabbit advanced atherosclerosis using ¹⁸F-fluoromisonidazole positron emission tomographic imaging. *Circ Cardiovasc Imaging*. 2014;7(2):312–20.
- Mirasol RV, Bokkers RP, Hernandez DA, et al. Assessing reperfusion with whole-brain arterial spin labeling: a noninvasive alternative to gadolinium. *Stroke*. 2014;45(2):456–61.
- Mueller S, Wang D, Fox MD, et al. Individual variability in functional connectivity architecture of the human brain. *Neuron*. 2013;77(3):586–95.
- Okazawa H, Higashino Y, Tsujikawa T, et al. Noninvasive method for measurement of cerebral blood flow using O-15 water PET/MRI with ASL correlation. *Eur J Radiol*. 2018;105:102–9.
- Park CH, Chang WH, Ohn SH, et al. Longitudinal changes of resting-state functional connectivity during motor recovery after stroke. *Stroke*. 2011;42(5):1357–62.
- Powers WJ, Clarke WR, Grubb RL, et al. Extracranial-intracranial bypass surgery for stroke prevention in hemodynamic cerebral ischemia. *JAMA*. 2011;306(18):1983–92.
- Puig O, Henriksen OM, Vestergaard MB, et al. Comparison of simultaneous arterial spin labeling MRI and ¹⁵O-H₂O PET measurements of regional cerebral blood flow in rest and altered perfusion states. *J Cereb Blood Flow Metab*. 2020;40(8):1621–33.
- Quality Management and Safety Management Group of the Chinese Society of Radiology, Magnetic Resonance Group of the Chinese Society of Radiology. Expert consensus on the standardized application of arterial spin labelling cerebral perfusion MRI. *Chin J Radiol*. 2016;50(11):817–24.
- Reynolds MR, Derdeyn CP, Grubb RL, et al. Extracranial-intracranial bypass for ischemic cerebrovascular disease: what have we learned from the Carotid Occlusion Surgery Study? *Neurosurg Focus*. 2014;36(1):E9.
- Rudd JH, Warburton EA, Fryer TD, et al. Imaging atherosclerotic plaque inflammation with [¹⁸F]-Fluorodeoxyglucose positron emission tomography. *Circulation*. 2002;105(23):2708–11.
- Saba L, Anzidei M, Marincola BC, et al. Imaging of the carotid artery vulnerable plaque. *Cardiovasc Inter Rad*. 2014;37(3):572–85.
- Sebok M, Van Niftrik CHB, Piccirelli M, et al. BOLD cerebrovascular reactivity as a novel marker for crossed cerebellar diaschisis. *Neurology*. 2018;91(14):e1328–37.
- Shen K, Hutchison RM, Bezgin G, et al. Network structure shapes spontaneous functional connectivity dynamics. *J Neurosci*. 2015;35(14):5579–88.
- Small SL, Hlustik P, Noll DC, et al. Cerebellar hemispheric activation ipsilateral to the paretic hand correlates with functional recovery after stroke. *Brain*. 2002;125(7):1544–57.
- Su Y, Arbelaez AM, Benzinger TL, et al. Noninvasive estimation of the arterial input function in positron emission tomography imaging of cerebral blood flow. *J Cereb Blood Flow Metab*. 2012;33(1):115–21.
- Su Y, Vlassenko AG, Couture LE, et al. Quantitative hemodynamic PET imaging using image-derived arterial input function and a PET/MR hybrid scanner. *J Cereb Blood Flow Metab*. 2017;37(4):1435–46.
- Su Y, Wang H, Liang Z, et al. Evaluation of cerebrovascular reserve in patients with unilateral internal carotid artery or middle cerebral artery stenosis: A study on ¹⁵N-Ammonia PET/CT cerebral perfusion imaging combined with methazolamide challenge. *Chin J Rehabil Theory Pract*. 2016;22(11):1304–9.
- Van Golen LW, Kuijper JPA, Huisman MC, et al. Quantification of cerebral blood flow in healthy volunteers and type 1 diabetic patients: comparison of MRI arterial spin labeling and [¹⁵O]H₂O positron emission tomography (PET). *J Magn Reson Imaging*. 2014;40(6):1300–9.
- Vesey AT, Jenkins W, Forsythe R, et al. ¹⁸F-Fluoride and ¹⁸F-Fluorodeoxy- glucose positron emission tomography after transient ischemic attack or minor ischemic stroke: case-control study. *J Am Coll Cardiol*. 2016;67(13):1616.
- Walberer M, Backes H, Rueger MA, et al. Potential of early [¹⁸F]-2-Fluoro-2-Deoxy-D-Glucose positron emission tomography for identifying hypoperfusion and predicting fate of tissue in a rat embolic stroke model. *Stroke*. 2012;43(1):193–8.
- Wang M, Ma Y, Ji X, et al. Imaging characteristics and patterns of simultaneous cerebral metabolism and cerebral blood flow imaging in ischemic cerebrovascular disease. *J Capital Med Univ*. 2013;34(1):43–8.
- Wang J, Yang Z, Zhang M, et al. Disrupted functional connectivity and activity in the white matter of the sen-

- sensorimotor system in patients with pontine strokes. *J Magn Reson Imaging*. 2019;49(2):478–86.
- Wang L, Yu C, Chen H, et al. Dynamic functional reorganization of the motor execution network after stroke. *Brain*. 2010;133(Pt 4):1224–38.
- Xu HJ, Qin W, Chen H, et al. Contribution of the resting-state functional connectivity of the contralateral primary sensorimotor cortex to motor recovery after subcortical stroke. *PLoS One*. 2014;9(1):e84729.
- Yin L, Cheng S, Xiao J, et al. 3D pseudocontinuous arterial spin-labeling perfusion imaging detected crossed cerebellar diaschisis in acute, subacute and chronic intracerebral hemorrhage. *Clin Imaging*. 2018;50:37–42.
- Yu Z, Shi X, Zhou Z, et al. Cerebral glucose metabolism changes in chronic ischemia patients following subcranial-intracranial bypass. *Neurosurg Rev*. 2020;43(5):1383–9.
- Zaro-Weber O, Moeller-Hartmann W, Siegmund D, et al. MRI-based mismatch detection in acute ischemic stroke: optimal PWI maps and thresholds validated with PET. *J Cereb Blood Flow Metab*. 2017;37(9):3176–83.
- Zhang M, Lu J, Jiao L, et al. Proton magnetic resonance spectroscopy in patients with symptomatic unilateral internal carotid artery/middle cerebral artery stenosis or occlusion. *J Magn Reson Imaging*. 2011;34(4):910–6.